AD/A-005 271

A PARACHUTE OPENING SHOCK THEORY BASED ON NON LINEAR TIME HISTORIES OF INFLOW VELOCITY AND PROJECTED AREA

Helmut G. Heinrich, et al

Minnesota University

Prepared for:

Army Natick Laboratories

June 1974

TECHNICAL REPORT
75-10 AMEL

A PARACHUTE OPENING SHOCK THEORY BASED ON NON LINEAR TIME HISTORIES OF INFLOW VELOCITY AND PROJECTED AREA

by

Helmut G. Heinrich

Robert A. Noreen
and

David P. Saari

University of Minnesota
Minneapolis, Minnesota

Contract Number: DAAG17-73-C-0174

May 1974

UNITED STATES ARMY
NATICK LABORATORIES
Natick, Massachusetts 01760

U.S. ARMY TROOP SUPPORT COMMAND

Aero-Mechanical Engineering Laboratory

Approved for public release; distribution unlimited.

Citation of trade names in this report does not constitute an official indorsement or approval of the use of such items.

Destroy this report when no longer needed. Do not return it to the originator.

SECURITY CLASSIFICATIDN DF THIS PAGE *(When Dete Entered)*

REPORT DOCUMENTATION PAGE

READ INSTRUCTIONS BEFORE COMPLETING FORM

1. REPDRT NUMBER: AMEL 75-10	2. 3DVT ACCESSIDN ND.
3. RECIPIENT'S CATALDG NUMBER: AD/A-005 271	
4. TITLE *(and Subtitle)*: A Parachute Opening Shock Theory Based on Non-Linear Time Histories of Inflow Velocity and Projected Area.	5. TYPE DF REPORT & PERIOD COVERED: Final, April 1973 - June 1974
	6. PERFORMING DRG. REPDRT NUMBER
7. AUTHDR(s): Helmut G. Heinrich, Robert A. Noreen, David P. Saari	8. CDNTRACT DR GRANT NUMBER(s): DAAG 17-73-C-0174
9. PERFORMING DRGANIZATIDN NAME AND ADDRESS: University of Minnesota, Department of Aeronautics and Engineering Mechanics, Minneapolis, Minnesota 55455	10. PRDGRAM ELEMENT, PRDJECT, TASK AREA & WORK UNIT NUMBERS: 62203A, 1F162203AH86, 04, 032
11. CDNTRDLLING OFFICE NAME AND ADDRESS: US Army Natick Laboratories, Airdrop Engineering Laboratory STSNL-AAP, Natick, Massachusetts 01760	12. REPDRT DATE: June 1974
	13. NUMBER DF PAGES: 85
14. MONITORING AGENCY NAME & ADDRESS *(if different from Controlling Office)*	15. SECURITY CLASS. *(of this report)*: UNCLASSIFIED
	15a. DECLASSIFICATION/DOWNGRADING SCHEDULE

16. DISTRIBUTION STATEMENT *(of this Report)*

Approved for public release; distribution unlimited.

17. DISTRIBUTIDN STATEMENT *(of the abstract entered in Block 20, if different from Report)*

This document has been approved for public release and sale; its distribution is unlimited.

18. SUPPLEMENTARY NDTES

19. KEY WDRDS *(Continue on reverse side if necessary and identify by block number)*

Parachute
Opening (Process)
Opening Force
Shock
Functions (Mathematics)
Area
Velocity

20. ABSTRACT *(Continue on reverse side if necessary and identify by block number)*

The concept of a parachute opening shock calculation is shown which is based on the simultaneous solution of the equation of motion and the continuity equation with numerical inputs concerning the development of the projected area and the inflow velocity. Several area-time and velocity-time functions were extracted from wind tunnel and field test data and used for calculating a variety of test cases for which force-time recordings were available.

DD FDRM 1 JAN 73 1473 EDITIDN OF 1 NDV 65 IS OBSOLETE

SECURITY CLASSIFICATION OF THIS PAGE *(When Dete Entered)*

20. Abstract (Cont'd):

When these functions were used to calculate force-time histories for the test cases from which they were extracted, the calculated histories matched closely the measured ones. A unique set of functions was not found; however, one set was established which in many cases provided acceptable predictions of maximum forces and force-time shapes for parachutes of 3 ft to 100 ft diameter and velocities between 50 ft/sec and 300 ft/sec.

Another set of functions, closely related to the one covering the wide range, was established which matched the large parachutes particularly well.

Distribution of this
document is unlimited

AD_____

TECHNICAL REPORT

75-10 AMEL

A PARACHUTE OPENING SHOCK THEORY BASED ON NON-LINEAR TIME HISTORIES OF INFLOW VELOCITY AND PROJECTED AREA

by

Helmut G. Heinrich
Robert A. Noreen
David P. Saari

University of Minnesota
Minneapolis, Minnesota USA

Contract No. DAAG17-73-C-0174

Project Reference: 1F162203AH86

Airdrop Engineering Laboratory
U. S. ARMY NATICK LABORATORIES
Natick, Massachusetts 01760

FOREWORD

This work was performed under US Army Natick Laboratories Contract No. DAAG 17-73-C-0174 during the period of 20 April 1973 and 30 June 1974. The Project Number was 1F162203AH86, "Exploratory Development of Airdrop Systems". The Task No. was 04 and the Work Unit No. was 032 titled "Opening Performance of Large Cargo Parachutes". Mr. Edward J. Giebutowski of the Airdrop Engineering Laboratory served as the Project Officer.

The purpose of this effort was to improve the predictability of the opening performance of large cargo parachutes as used by the US Army.

CONTENTS

ILLUSTRATIONS

ILLUSTRATIONS (CONT.)

ILLUSTRATIONS (CONT.)

TABLES

SYMBOLS

C_D	drag coefficient
C_DS	drag area
$(C_DS)_i$	initial parachute drag area
D	diameter
d	inlet diameter
F	opening force
F_{max}	maximum opening force
g	acceleration due to gravity
L_s	suspension line length
m	mass
S	area
T	dimensionless time
t	time
u	outflow velocity
u/v	effective porosity
V	volume
v	velocity
v_{in}*	net inflow velocity
W	weight
θ	trajectory angle
ρ	air density

Subscripts:

a	apparent
f	filling
i	included
in	inflow, inlet
ℓ	load
max	value at T = 1.0, when used with D_p, S_p, V
o	initial, nominal
p	projected, parachute
s	snatch
ss	suspension system
T	total

ABSTRACT

The concept of a parachute opening shock calculation is shown which is based on the simultaneous solution of the equation of motion and the continuity equation with numerical inputs concerning the development of the projected area and the inflow velocity. Several area-time and velocity-time functions were extracted from wind tunnel and field test data and used for calculating a variety of test cases for which force-time recordings were available.

When these functions were used to calculate force-time histories for the test cases from which they were extracted, the calculated histories closely matched the measured ones. A unique set of functions was not found; however, one set was established which in many cases provided acceptable predictions of maximum forces and force-time histories for parachutes of 3 ft to 100 ft diameter and velocities between 50 ft/sec and 300 ft/sec.

Another set of functions, closely related to the one covering the wide range, was established which matched the large parachutes particularly well.

I. INTRODUCTION

The performance of an inflating parachute is governed by a complex interaction of aerodynamic, dynamic, and elastic forces. Seeking to analyze the opening process and to predict the opening force has been a problem of continuing interest. The first known analysis was published in 1927 (Ref 1) and was followed by a considerable number of other attempts and Refs 2 through 18 are merely a sample listing. To date, the most extensive study in which maximum calculated opening forces of solid cloth parachutes are compared with field test data is presented in Ref 19. In this study opening forces were calculated and compared with field test results for a 28 ft solid flat circular parachute under various surface loadings, speeds, and altitudes, and the results showed good agreement with the field test data.

The concept of the method used in Ref 19 was to calculate the instantaneous forces based on the continuity equation and the equation of motion considering the effective porosity of the parachute cloth and disregarding the effects of gravity upon the trajectory during the inflation process. Linear functions of the inflow velocity and the development of the projected area versus time were used as empirical inputs. Also, a mechanical model of the inflating canopy was chosen which consisted of a truncated cone capped by a hemisphere. This method gave good approximations of the measured maximum forces of the 28 ft solid flat parachute with 200 lb, 440 lb, and 820 lb suspended loads over a speed range of 150 ft/sec to 450 ft/sec and an altitude range of 6000 ft to 21,000 ft.

In Refs 20 and 21, the method of Ref 19 was used, but the equations of motion were expanded to include the effect of gravity upon the trajectory. The maximum forces calculated for the previously investigated cases of the 28 ft

parachute gave essentially the same results as shown in Ref 19. However, when this method was used for calculating opening forces of 64 ft parachutes with 2,200 lb suspended loads, the calculated results differed significantly from field test measurements.

In the following, a method of opening force calculation is presented which is somewhat similar to the one of Ref 19, however, the functions of inflow velocity and area development are non-linear with respect to time and reflect more realistically the events which occur during the inflation of the parachute canopy. Basically they are extracted from available field test data.

When the area and inflow functions were extracted from a particular test and introduced in the system of equations, the calculations provided force-time histories which very closely matched the field test recordings of that particular test. This is some proof that the method of calculation closely reflects the aerodynamics and dynamics of the inflation process.

An attempt was then made to find a set of unique functions which would be useful to calculate parachute opening processes of 3 ft to 100 ft parachutes. This attempt was partially successful, and characteristic functions were found, which, in connection with the established method, provide force-time histories of 3 ft, 28 ft, 64 ft, and 100 ft parachutes that match force-time recordings of actual tests with a reasonable degree of accuracy.

II. MODEL AND EQUATIONS FOR OPENING PERFORMANCE CALCULATIONS

As formulated in Ref 19 and revised in Ref 20, the motion of the parachute-load system during inflation is governed by the following equations:

$$\frac{dV}{dt} = \left(\frac{m_\ell + m_{ss} + m_p}{m_T}\right) g\cos\theta - \frac{\rho V^2 (C_o S_\ell + C_{Dp} \frac{\pi D_p^2}{4})}{2 m_T} \qquad (1)$$

$$- \frac{V}{m_T} \frac{1}{t_f} \left(\frac{dm_i}{dT} + \frac{dm_a}{dT}\right)$$

and

$$\frac{d\theta}{dt} = -\left(\frac{m_\ell + m_{ss} + m_p}{m_T}\right) \frac{g\sin\theta}{V} \qquad (2)$$

The filling time t_f follows from integration of the continuity equation, which can be expressed as

$$\frac{dV}{dt} = \pi V \left(\frac{V_{in}}{V} \frac{d^2}{4} - \frac{U}{V} \frac{D_p^2}{2}\right) \qquad (3)$$

The opening force, as stated in Ref 20, is

$$F = m_\ell \left(g\cos\theta - \frac{dV}{dt}\right) \qquad (4)$$

Thus a calculation of the opening performance of a parachute involves simultaneous solution of Eqns (1), (2), and (3) for t_f, v, and θ. The important variables for which functions must be formulated are the parachute area, the included and apparent masses, and the inflow velocity. A measured relationship for the projected canopy area, S_p, vs time coupled with idealized shapes will provide the means to evaluate all the variables but the inflow velocity.

A. Concept for Extraction of Inflow Functions

A method for extracting inflow functions from field test measurements was developed in a Master's Thesis by Uotila (Ref 22). The continuity equation may be written as

$$\frac{dV}{dt} = \frac{\pi d^2}{4} v_{in}^* \tag{5}$$

with v_{in}^* being a net inflow velocity which is essentially the value in parentheses, multiplied by the system velocity, v, of Eqn (3).

The system velocity, v, can be found from the relationship

$$v = \frac{t_f}{m_\ell} \int_0^T F dT \tag{6}$$

provided that t_f and F(T) are known.

The numerical values in Ref 22 were related to 28 ft solid flat parachutes obtained from the USAF data bank (Ref 23). In Ref 22, one particular test, USAF Test No. 44, was analyzed in detail. The suspended weight was 439 lb, the snatch velocity was 255 ft/sec and the altitude at snatch was 6075 ft. The filling time as defined in Ref 9 was t_f = 0.93 sec.

The force, taken from Ref 23, is shown vs dimensionless time in Fig 1, together with a 9th order least-squares polynomial approximation. This polynomial was used to find an approximation to the system velocity, assuming horizontal flight. The resulting system velocity, nondimensionalized by the snatch velocity, is shown in Fig 2.

From the same test, the area-time data is shown in Fig 3, including a numerical approximation as well as an average suggested in Ref 9.

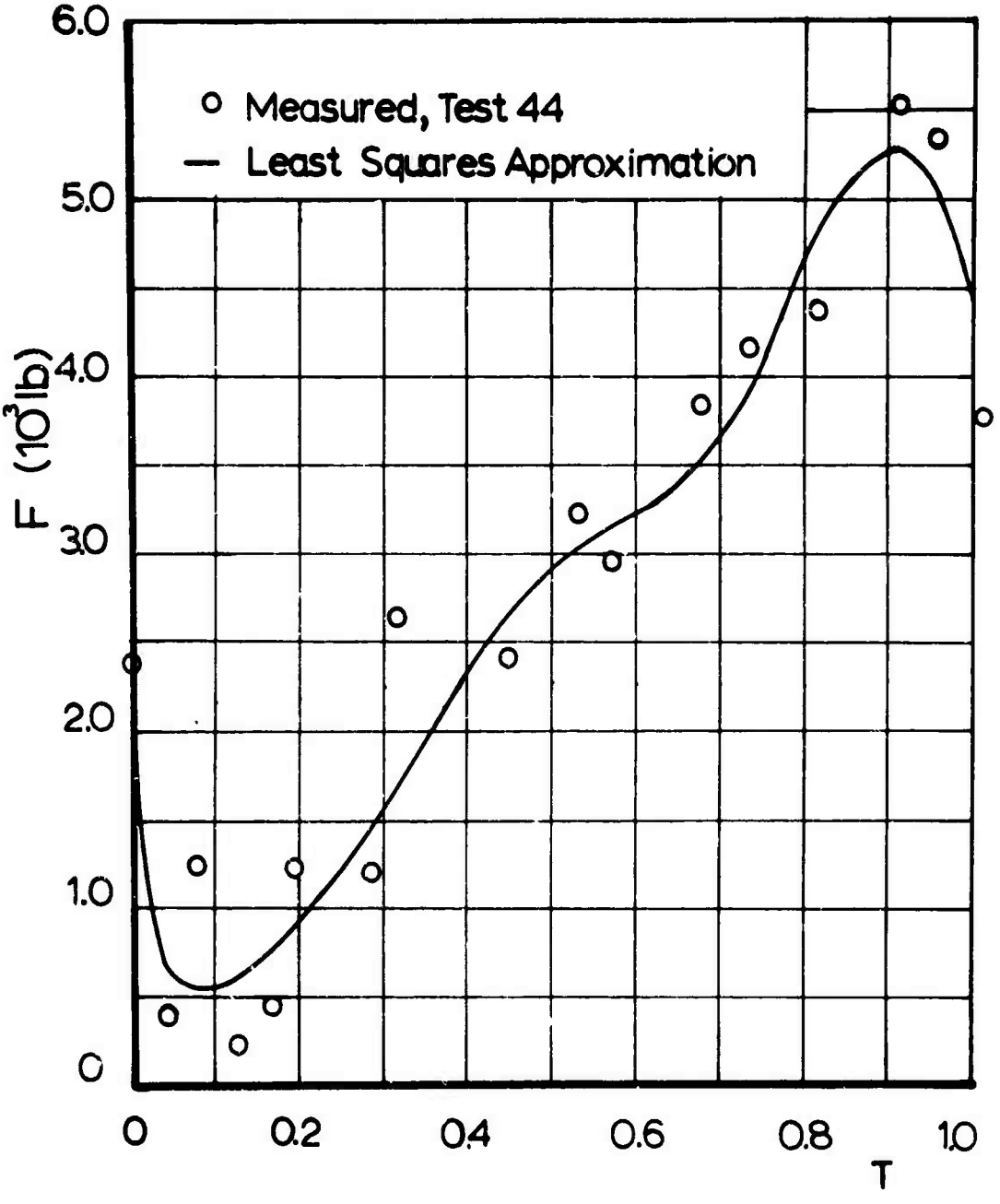

Fig 1 Force - Time History for C-9 Parachute, Test 44, V_s = 255 ft/sec, W_1 = 4391b

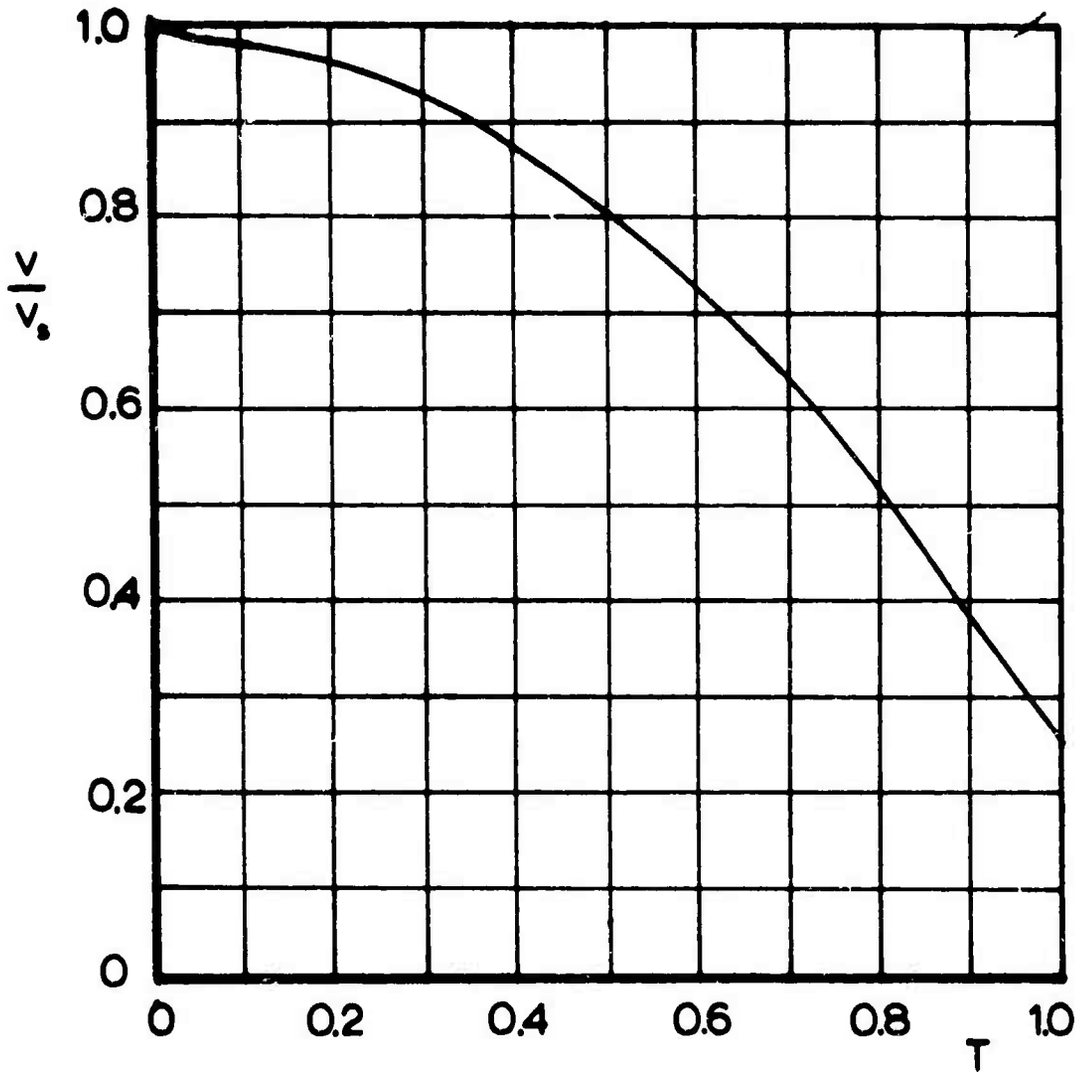

Fig 2 System Velocity Ratio Based on Force Approximation (Fig 1)

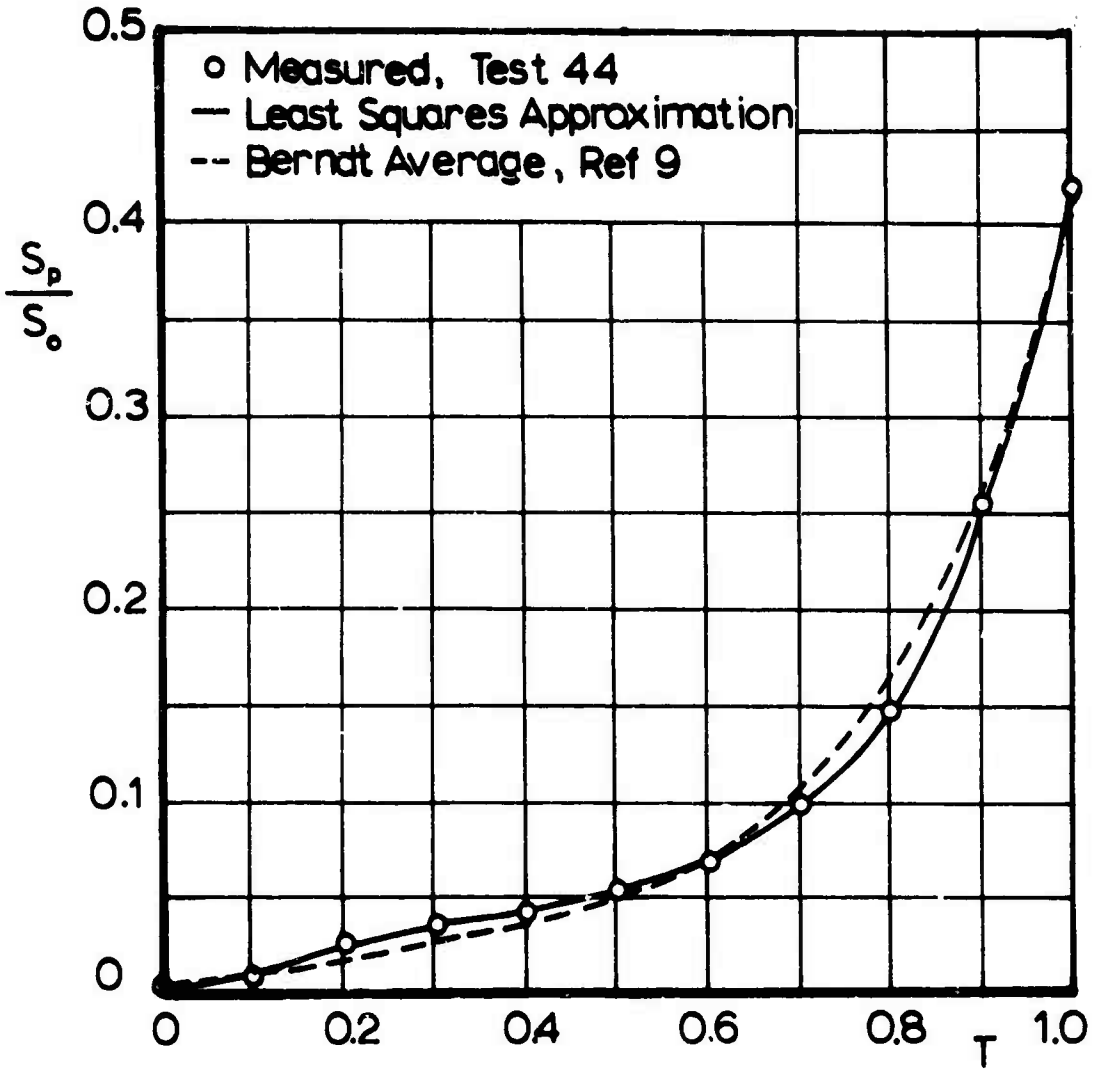

Fig 3 Area-Time Relationship for C-9 Parachute, Test 44

Assuming that the canopy profile is described by the so-called Minnesota shape, the volume of the canopy is given by (Ref 22)

$$\frac{V}{V_{max}} = \frac{\pi^3}{8}\left\{\frac{S_p}{S_o}\sqrt{\left(\frac{3}{2}-\frac{\pi}{4}\frac{D_p}{D_o}\right)^2-\frac{1}{4}\frac{S_p}{S_o}} - \frac{S_{in}}{S_o}\sqrt{1-\frac{1}{4}\frac{S_{in}}{S_o}+\left(\frac{D_p}{D_o}\right)^3}\right\} \tag{7}$$

where

$$V_{max} = \frac{\pi}{12}\left(D_{P_{max}}\right)^3 \tag{8}$$

$$S_{in} = \frac{\pi d^2}{4} \tag{9}$$

In Eqn (7) it is assumed that $L_s = D_o$ for simplicity. With some suitable expansion, Eqn (5) provides the inflow velocity

$$V_{in}^* = \frac{V_{max}}{t_f S_o}\ \frac{S_o}{S_{in}}\ \frac{d}{d\tau}\left(\frac{V}{V_{max}}\right) \tag{10}$$

The area-time history, Fig 3, combined with the mechanical model provides the time histories of the normalized inlet area, Fig 4, and combined with Eqn (7) gives the volume-time and finally the volume derivative-time function, Fig 5.

From Eqn 10 combined with the numerical approximations to time histories of the area and volume follows the net inflow velocity v_{in}^* as shown in Fig 6.

A dimensionless inflow function can then be formed

$$\frac{V_{in}^*}{V} = \frac{V_{max}}{V_o t_f S_o}\left(\frac{S_{in}}{S_o}\frac{V}{V_o}\right)^{-1}\ \frac{d}{d\tau}\left(\frac{V}{V_{max}}\right) \tag{11}$$

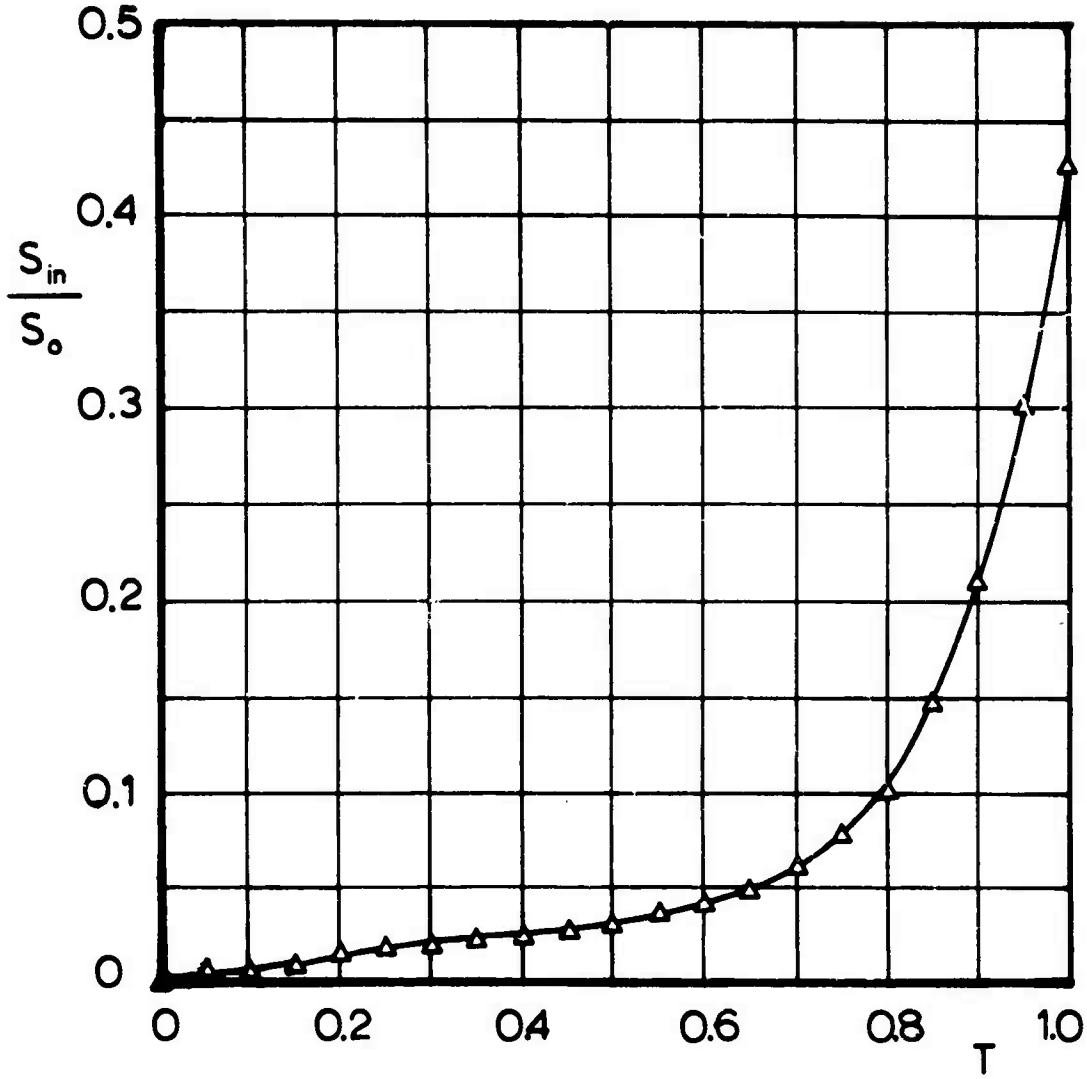

Fig 4 Inlet Area Ratio for Test 44, Based on Projected Area Approximation (Fig 3)

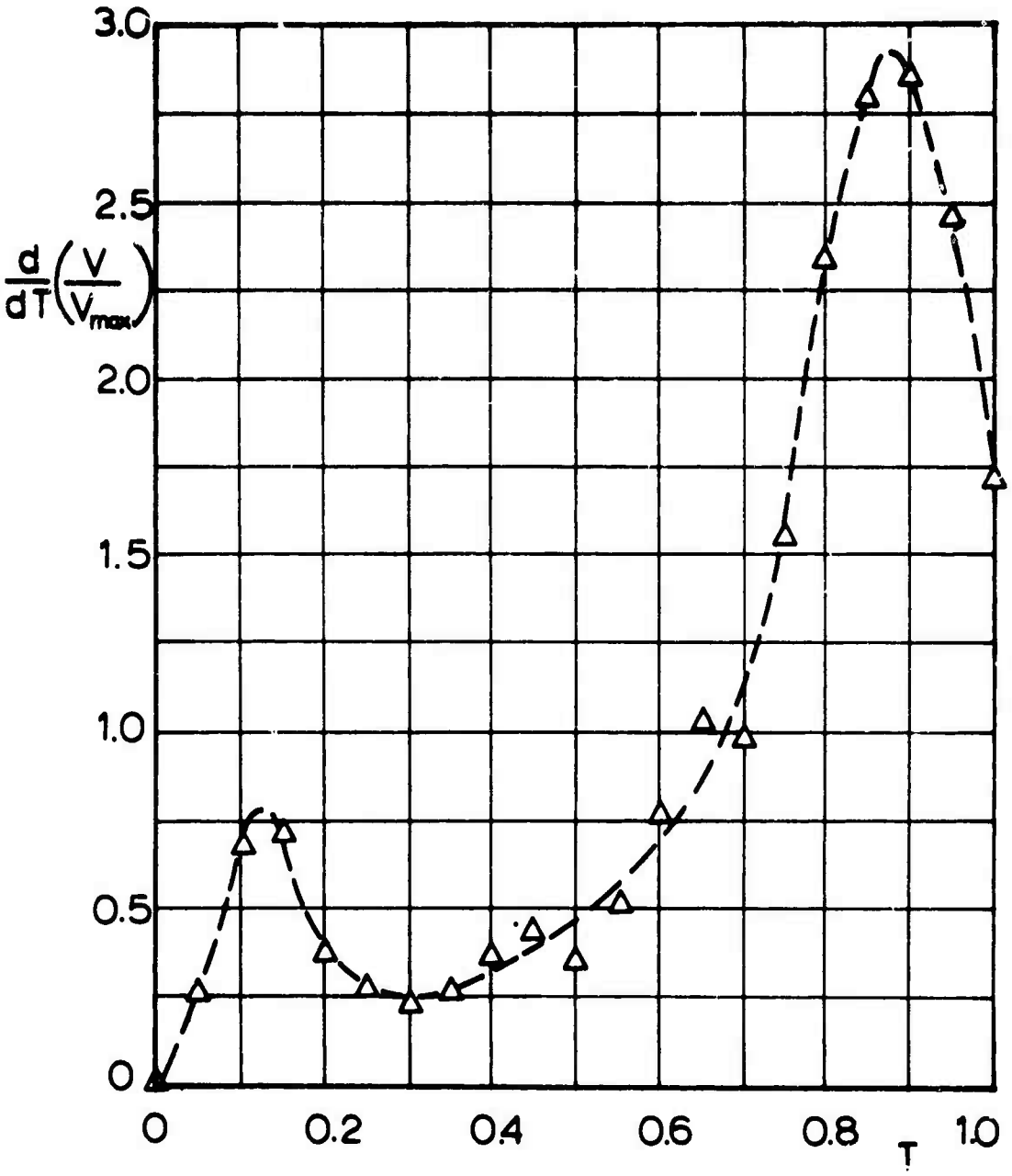

Fig 5 Dimensionless Volume Derivative for Test 44 Based on Area Approximation (Fig 3)

731 o

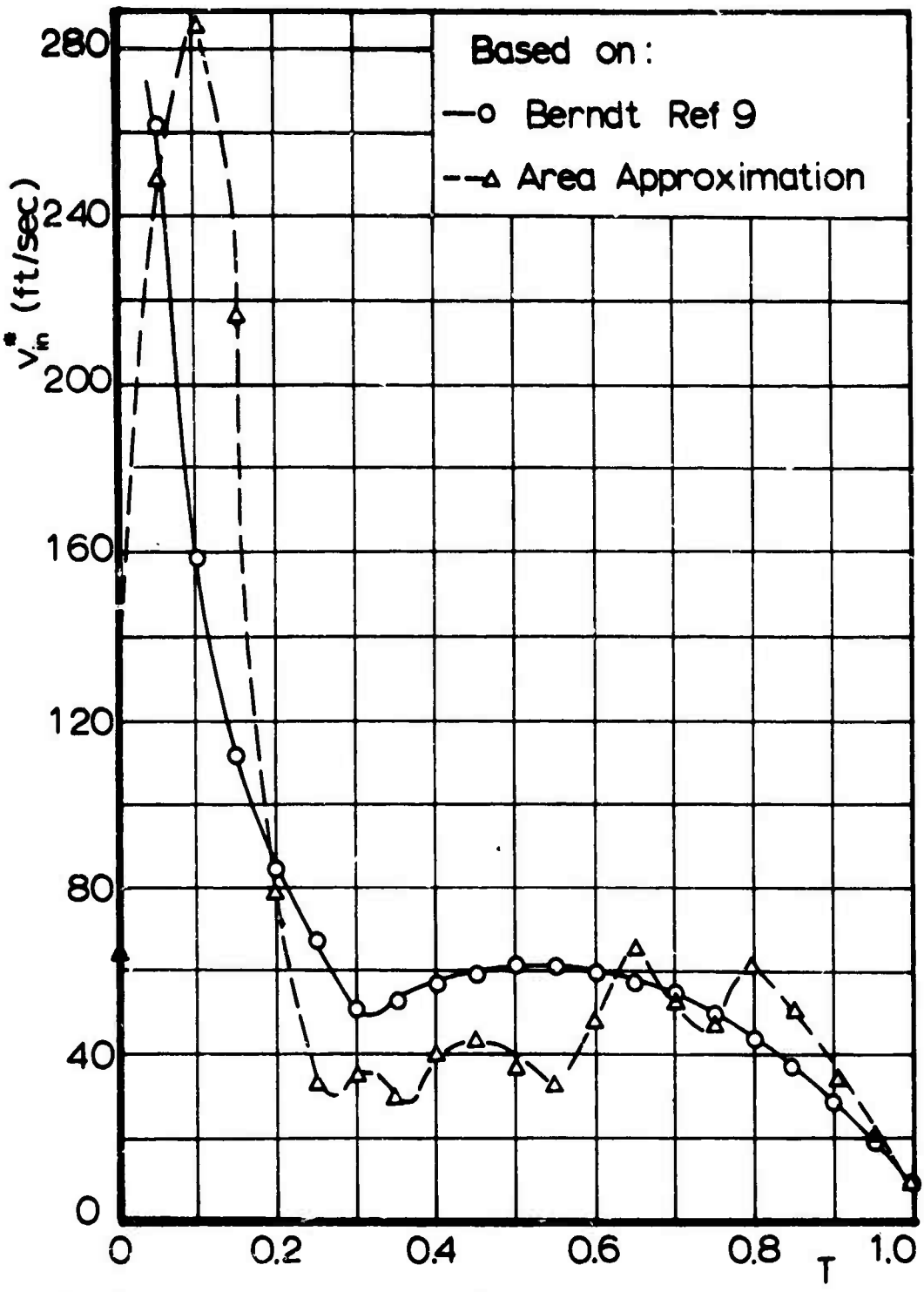

Fig 6 Net Inflow Velocity for Test 44, Based on Fig 3

which is shown in Fig 7. It should be kept in mind that all these derivations are made for USAF Test No. 44 (Ref 23). In Figs 3 and 6, Berndt's average (Ref 9) is used for comparative purposes and is specifically identified. The dashed curve near T = 0 in Fig 7 is drawn through $v_{in}^*/v = 1$ to comply with physical initial conditions.

With the time histories of the projected area, volume or mass, apparent mass, and velocity as well as the filling time, t_f, known, the instantaneous force can be calculated numerically from Eqns (1) and (4). If t_f is taken from Ref 23, it encompasses the time interval from the peak of the snatch force until the projected area of the inflating canopy equals that of the canopy during steady state descent. As pointed out in Ref 19, this period is, in general, not the time required by the continuity equation to establish an included air mass equal to the mass during steady state descent, because the filling of the canopy most probably does not begin at the instant of peak snatch force.

Figure 8 then indicates the force calculation using Eqn (4) and the data bank time of $t_f = 0.92$ sec. One notices a certain similarity of the general trend of the calculated and recorded forces; however, the maximum forces differ significantly.

As a next approximation, one may calculate a filling time by means of the inflow function, Fig 7, and one obtains a filling time of 0.76 sec. However, since the inflow function, Fig 7, was derived using the reported filling time, and this time should also be used in determing the mass derivatives dm_i/dt and dm_a/dt, the calculated force-time history using $t_f = 0.76$ sec must be considered to be merely an approximation. However, using this calculated filling time gives an agreement between measured and calculated force-time histories

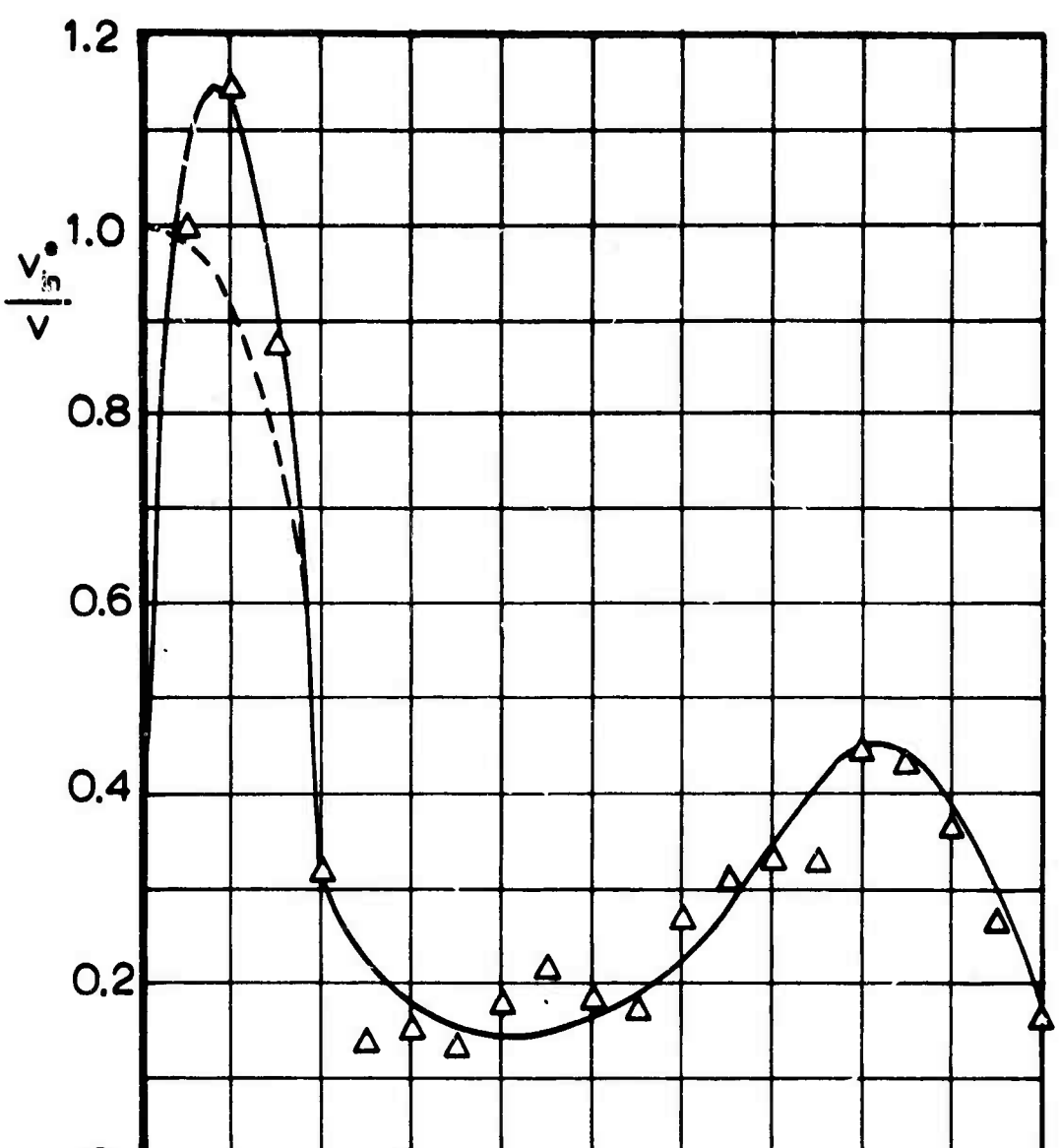

Fig 7 Net Inflow Function for Test 44, Based on Figs 2 and 6

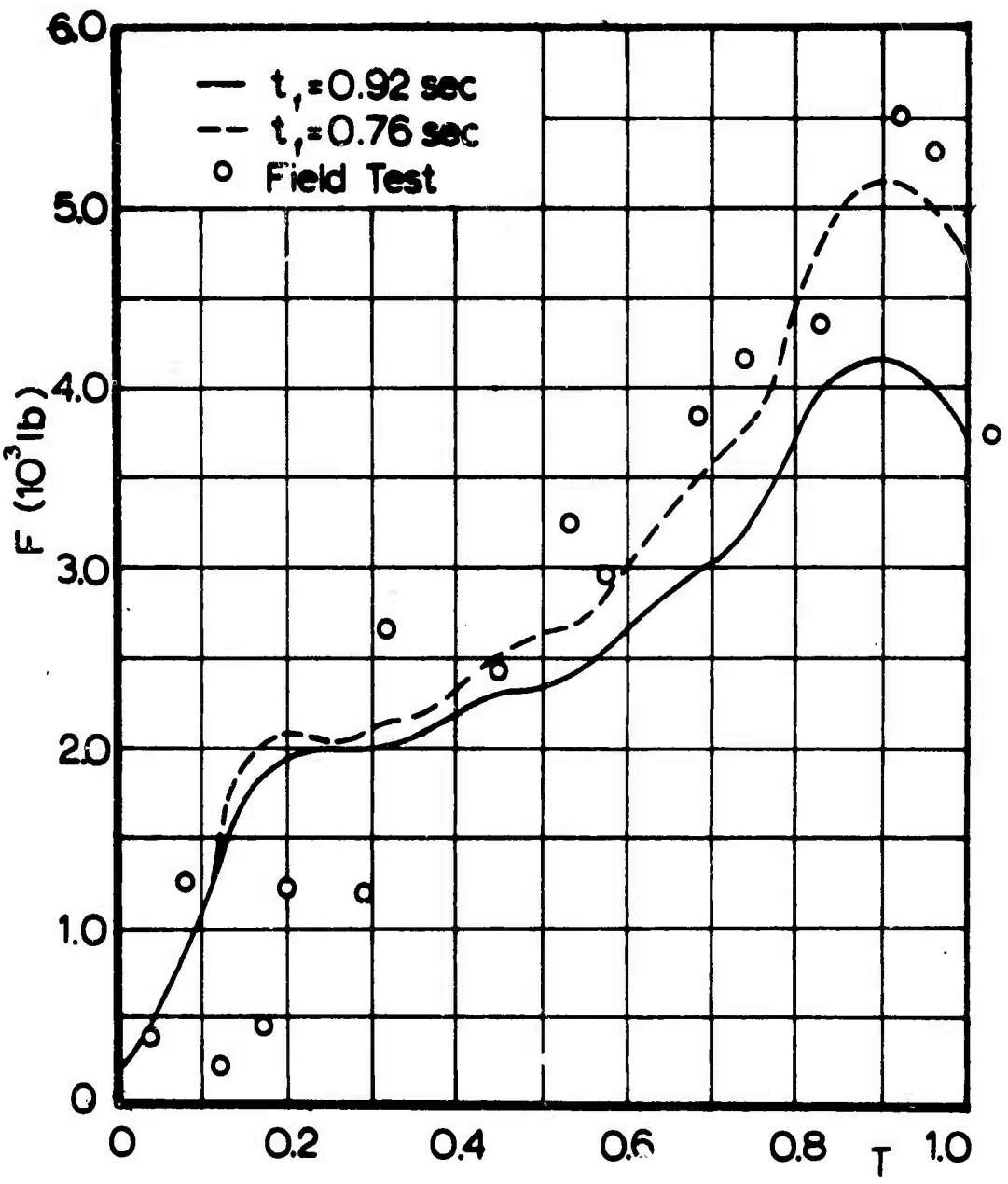

Fig 8 Calculated Force - Time Histories with t_1=0.92 sec and t_1=0.76 sec

which is very encouraging, and the method appears to deserve further refinement.

The simultaneous solution of the equations of motion and continuity with the removal of the inconsistency concerning the filling time will be discussed in the following.

B. The Terms of the Equations of Motion and Continuity

The preceding chapter indicates the strong influence of the filling time. Also, a meaningful opening shock calculation should not depend on a filling time selected from experience or available field test data with the hope of good luck. Therefore, an attempt will be made in the following to develop a method in which the final force-time history results from a simultaneous solution of the equation of motion and the continuity equation. The inputs concerning area-time and inflow-time functions shall be extracted from closely observed field tests and carefully considered boundary conditions. Also, the terms of aerodynamic drag, canopy volume, mass and apparent mass shall be reviewed.

1. Filling Time

The filling time as defined in Ref 9 is the time from peak snatch force until the instant the projected area first reaches its steady state value. Therefore, some of the snatch process, including any dynamic effects due to elasticity, as well as bag strip, breaking of tie cords, and other matters occur during the time period so defined. Therefore, during a certain portion of the filling time in accordance with Ref 9, the parachute is not inflating in the usual sense. Considering the parachute to contribute only drag during some initial period of the filling time thus seems a reasonable description of events. From field

test data, it is estimated that this period extends from $0 \leq T \leq 0.15$, and during this time Eqns (1) and (2) take the form of

$$\frac{dv}{dt} = g\cos\theta - \frac{\rho v^2[(C_DS)_l + (C_DS)_i]}{2(m_l + m_{ss} + m_p)} \tag{12}$$

and

$$\frac{d\theta}{dt} = -\frac{g\sin\theta}{v} \tag{13}$$

with $(C_DS)_i$ representing the initial drag area of the parachute.

2. Included and Apparent Masses

The second point of interest concerns the interpretation of the included and apparent masses. The physical meaning of the included mass is that mass of air which moves with the system at system velocity. For a fully inflated parachute, a reasonable approximation should be that the entire canopy volume consists of air which is at rest relative to the parachute, and thus the included mass at full inflation would be

$$m_i\Big|_{T=1} = \rho V_{max} \tag{14}$$

However, during the filling process there is an inflow to the canopy and the entire canopy volume as given by the canopy model (Ref 19) cannot contain stagnant air. The model and the shape of an inflating actual parachute suggests that the portion which appears like an air filled dome is most likely the portion of the canopy containing stagnant air. A function describing the volume of this portion of the canopy would thus seem to be an appropriate

formulation for included mass, i.e.

$$m_i = \frac{\rho V_{max}}{(D_{P_{max}})^3} D_P^3 \qquad (15)$$

Apparent mass is a means of representing a fluid dynamic force due to the change of kinetic energy of the external flow field. The formulation of apparent mass in earlier studies of opening processes is based on measurements made on a fully inflated parachute (Ref 8) with a coefficient that increases from zero to one as the parachute inflates. This coefficient introduces a variation of the apparent mass in accordance with the shape of the inflating canopy. It should be kept in mind that in the linearized opening shock theory (Ref 19), the area ratio, S_p/S_o, increased linearly and that the results of such calculations fit measured maximum forces quite well. Therefore, as a first approximation a similar approach is made; namely, a dependence of the apparent mass on the stagnant volume, and thus on the included mass, multiplied with an area ratio factor. If the measurements of Ref 8 are expressed in terms of the included mass and this factor, the apparent mass is

$$m_a = \frac{3}{8}\left(\frac{D_P}{D_{P_{max}}}\right)^2 m_i \qquad (16)$$

3. Shape Assumptions

Another reconsideration of the calculation model was concerned with the idealized shape assumption. The field test projected area measurements from Ref 23 indicate that the projected area at full inflation amounts to $S_{P_{max}} = (0.42)\ S_o$. The Minnesota shape model, which is used in several publications including Ref 19, requires that the projected area at full inflation amount to $S_{P_{max}} = (0.405)\ S_o$.

Using the Minnesota shape model with the measured area curves from Ref 23 would cause an inconsistency. Therefore, the idealized shape formulated to describe the latter stages of inflation in Ref 9 was used. Using $S_{p_{max}} = 0.42\ S_o$ and this profile of the inflating canopy, the volume of the inflating parachute amounts to

$$V = \frac{\pi}{12}\left\{(.661)D_p^3 + D_p^2\sqrt{\left(L_s + \frac{D_o}{2} - .665D_p\right)^2 - \frac{D_p^2}{4}}\right. \\ \left. - d^2\sqrt{L_s^2 - \frac{d^2}{4}}\right. \tag{17}$$

and the inlet diameter is

$$d = \frac{L_s D_p}{L_s + \frac{D_o}{2} - .665D_p} \tag{18}$$

4. Canopy Volume

From the interpretation of the included mass in the equation of motion and the imbalance of the inflow and outflow in the continuity equation, it follows that there has to be a distinction between the canopy volume and the "included" volume. Consequently, the canopy volume has to be calculated from Eqns (17) and (18) whereas the included mass follows from Eqn (15).

5. Drag Coefficient

In earlier studies, for example Ref 19, it was assumed that the drag coefficient of the inflating canopy could be assumed to be constant when related to the cloth area of the inflated portion of the canopy. This assumption was reconsidered and sample calculations showed that a varying drag coefficient caused such a small variation of the total canopy force that the refinement did not justify the added

complication. Therefore, in all following calculations a constant drag coefficient of $C_{D_p} = 1.786$ was used (Ref 20).

C. Opening Performance Calculation Method

From the preceding discussion the numerical inputs for a calculation of the opening performance of a parachute are the descriptions of the projected area and inflow velocity as functions of dimensionless time as well as the physical data of the parachute-load system and the initial conditions.

The principle of extracting area and inflow velocity functions for use with this calculation method has been discussed in Section IIA. However, due to the various refinements since adopted, a brief summary is given below.

The inlet area $\pi d^2/4$ is derived from the projected area test records. The inflow velocity then follows from the derivative of the volume, Eqn (5).

During the time period $0 \leq T < 0.15$, the motion of the system follows from Eqns (12) and (13), and no inflow function is needed. For a computer program, the inflow function during this interval is set to zero.

For the period $0.15 \leq T \leq 1.0$, the inflow velocity follows from the derivative of Eqn (17) and is given by

$$V_{in}^* = \frac{1}{3d^2}\frac{1}{t_f}\left\{1.983 D_p^2 \frac{dD_p}{dT} + 2D_p\sqrt{\left[L_{ss}+\frac{D_o}{2}-(.665)D_p\right]^2-\frac{D_p^2}{4}}\ \frac{dD_p}{dT}\right.$$

$$+ D_p^2\ \frac{\left[-1.32\left(L_{ss}+\frac{D_o}{2}-.665\right)-\frac{D_p}{2}\right]}{2\sqrt{\left[L_{ss}+\frac{D_o}{2}-(.665)D_p\right]^2-\frac{D_p^2}{4}}}\ \frac{dD_p}{dT} \qquad (19)$$

$$\left. - 2d\sqrt{L_{ss}^2-\frac{d^2}{4}}\ \frac{d(d)}{dT} + \frac{d^3}{4\sqrt{L_{ss}^2-\frac{d^2}{4}}}\ \frac{d(d)}{dT}\right\}$$

The inflow function is then v_{in}^*/v, where v is determined from the equations of motion in conjunction with a specified filling time.

The opening force for a given parachute application, following this method, is found by solving the following equations:

For $0 \leq T < 0.15$:

$$\frac{dv}{dt} = g\cos\theta - \frac{\rho v^2[C_D S_\ell + (C_D S)_i]}{2(m_\ell + m_{ss} + m_P)} \tag{20}$$

$$\frac{d\theta}{dt} = -\frac{g\sin\theta}{v} \tag{21}$$

and for $T \geq 0.15$

$$\frac{dv}{dt} = \left(\frac{m_\ell + m_{ss} + m_P}{m_T}\right) g\cos\theta - \frac{\rho v^2\left(C_D S_\ell + C_{D_P}\frac{\pi D_P^2}{4}\right)}{2m_T}$$

$$- \frac{v}{m_T}\frac{1}{t_f}\left[\frac{dm_i}{dT} + \frac{dm_a}{dT}\right] \tag{22}$$

$$\frac{d\theta}{dt} = -\left(\frac{m_\ell + m_{ss} + m_P}{m_T}\right)\frac{g\sin\theta}{v} \tag{23}$$

where

$$m_i = \frac{\rho V_{max}}{(D_{P_{max}})^3} D_p^3 \tag{24}$$

$$m_a = \frac{3}{8}\left(\frac{D_p}{D_{P_{max}}}\right)^2 m_i \tag{25}$$

$$m_T = m_l + m_{ss} + m_p + m_i + m_a \tag{26}$$

The continuity equation is, in integral form,

$$V_{max} - V_{T=0.15} = t_f \int_{0.15}^{1} \frac{\pi d^2}{4}\left(\frac{V_{in}^*}{V}\right) v\, dT \tag{27}$$

Thus the parachute is assumed to inflate from an initial volume to a final volume during the period $0.15 \leq T \leq 1.0$. The initial, very small volume of air is assumed to be captured instantaneously and is found from the equations describing the idealized shape at $T = 0.15$.

The volume and inlet diameter are given by Eqns (17) and (18). The filling time is found by selecting values for t_f and solving Eqns (20) through (23) until Eqn (27) is satisfied. Once the filling time is known, the motion is found from Eqns (20) through (23), and the opening force is given by

$$F = m_l\left(g\cos\theta - \frac{dv}{dt}\right) \tag{28}$$

III. ANALYSIS OF INDIVIDUAL TEST CASES

To examine the suitability of the calculation method, several opening performance calculations were made using data related to a number of parachute drops and wind tunnel tests for which simultaneous measurements of opening force, projected area, and filling time were available. These individual tests represented a wide range of surface loadings and initial conditions. As the first step, a net inflow function was calculated for each case, using the data, initial conditions, the area curve, and the filling time from the measurements of the particular test. The next step was to perform a calculation of the opening force, using as inputs the measured area curve and the calculated inflow function.

These calculations were made for three wind tunnel tests of a 3 ft model parachute with a 0.5 lb suspended load (Ref 24), two airdrops of a 28 ft solid flat circular parachute with 200 lb suspended load (Ref 23) and three airdrops of a 28 ft parachute with a 439 lb load (Ref 23). The value of $(C_D S)_i$ in Eqn (19) was selected as

$$(C_D S)_i = (0.01) C_{D_p} S_{P_{max}} \tag{29}$$

based on an examination of Ref 25. In all cases, the filling time determined by integrating the continuity equation using the calculated inflow functions differed from the measured values by less than 2%. This indicates that the numerical procedures used for extraction of inflow functions from measured data are sufficiently accurate.

The results of the force calculations are shown in Figs 9 through 16. Note that although dimensionless filling time is plotted, since the filling times differ by less than 2%, the real time comparison would be essentially the same.

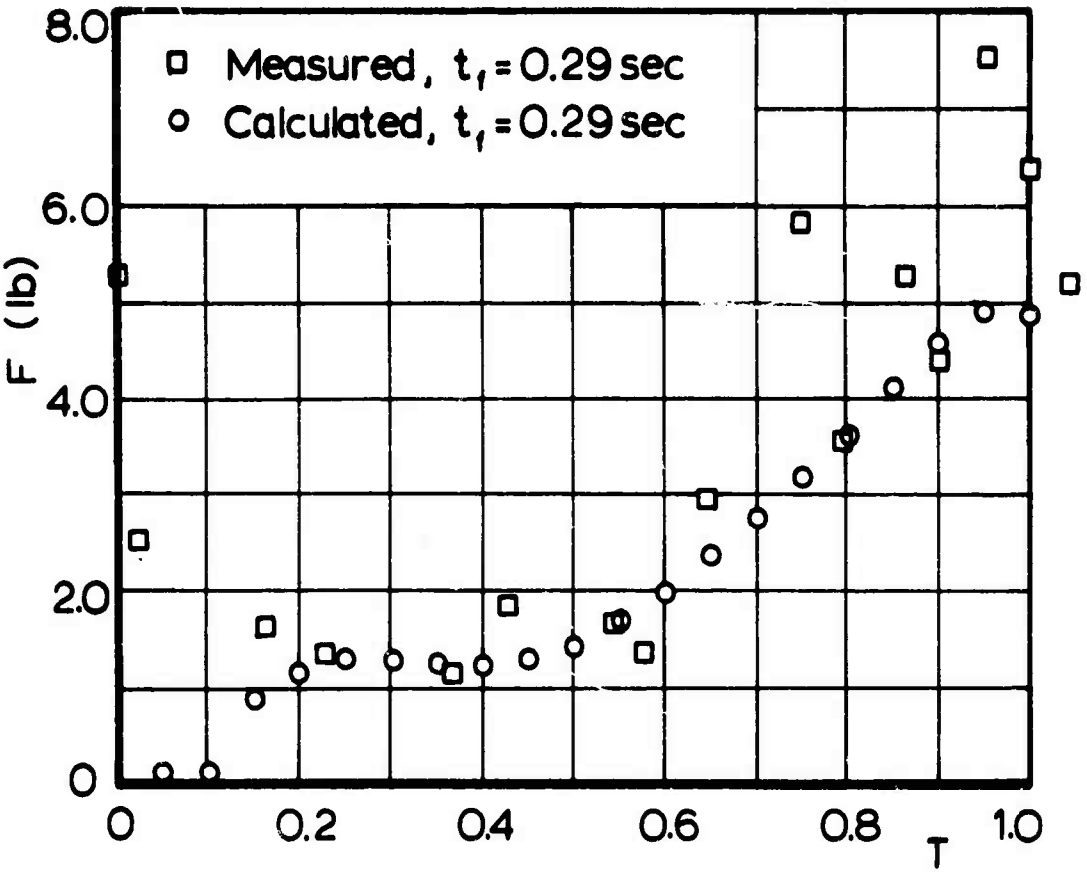

Fig 9 Calculated and Measured Force-Time Histories for a 3 ft Model Parachute, Test 2, $v_s = 50$ ft/sec, $W_1 = 0.5$ lb

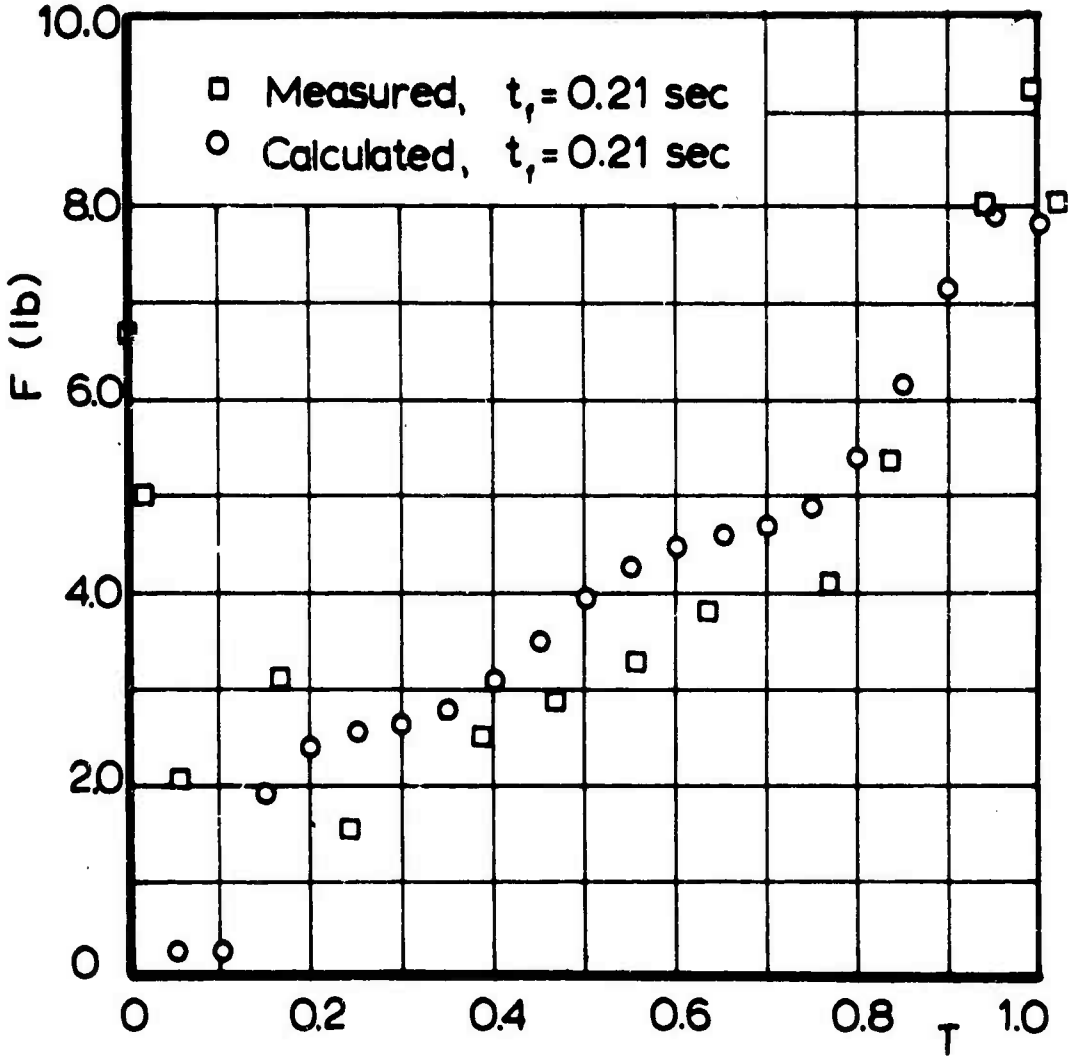

Fig 10 Calculated and Measured Force-Time Histories for a 3ft Model Parachute, Test 6, $V_s = 70$ ft/sec, $W_s = 0.5$ lb

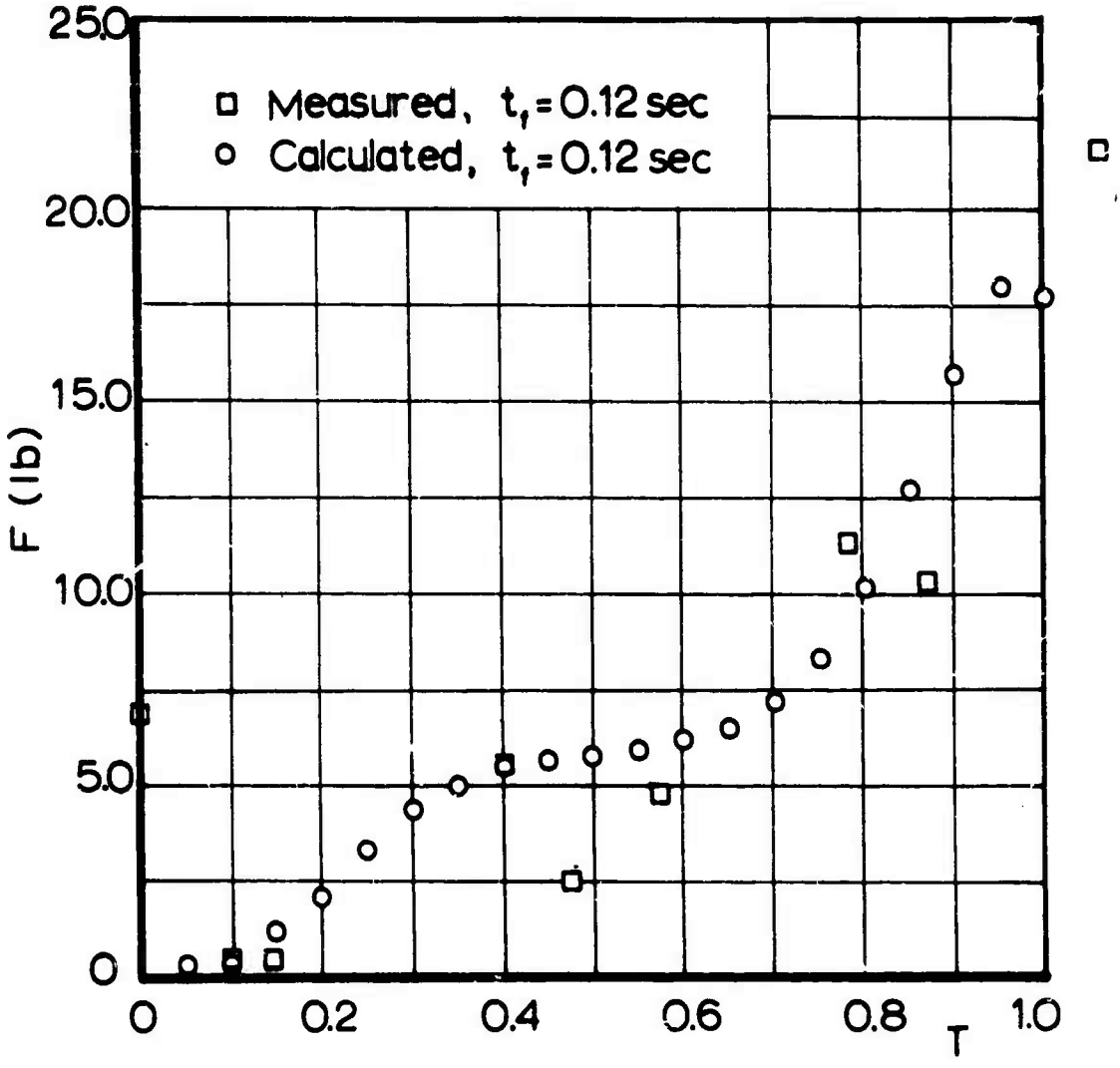

Fig 11 Calculated and Measured Force-Time Histories for a 3 ft Model Parachute, Test 10, $v_s = 85$ ft/sec, $W_1 = 0.5$ lb

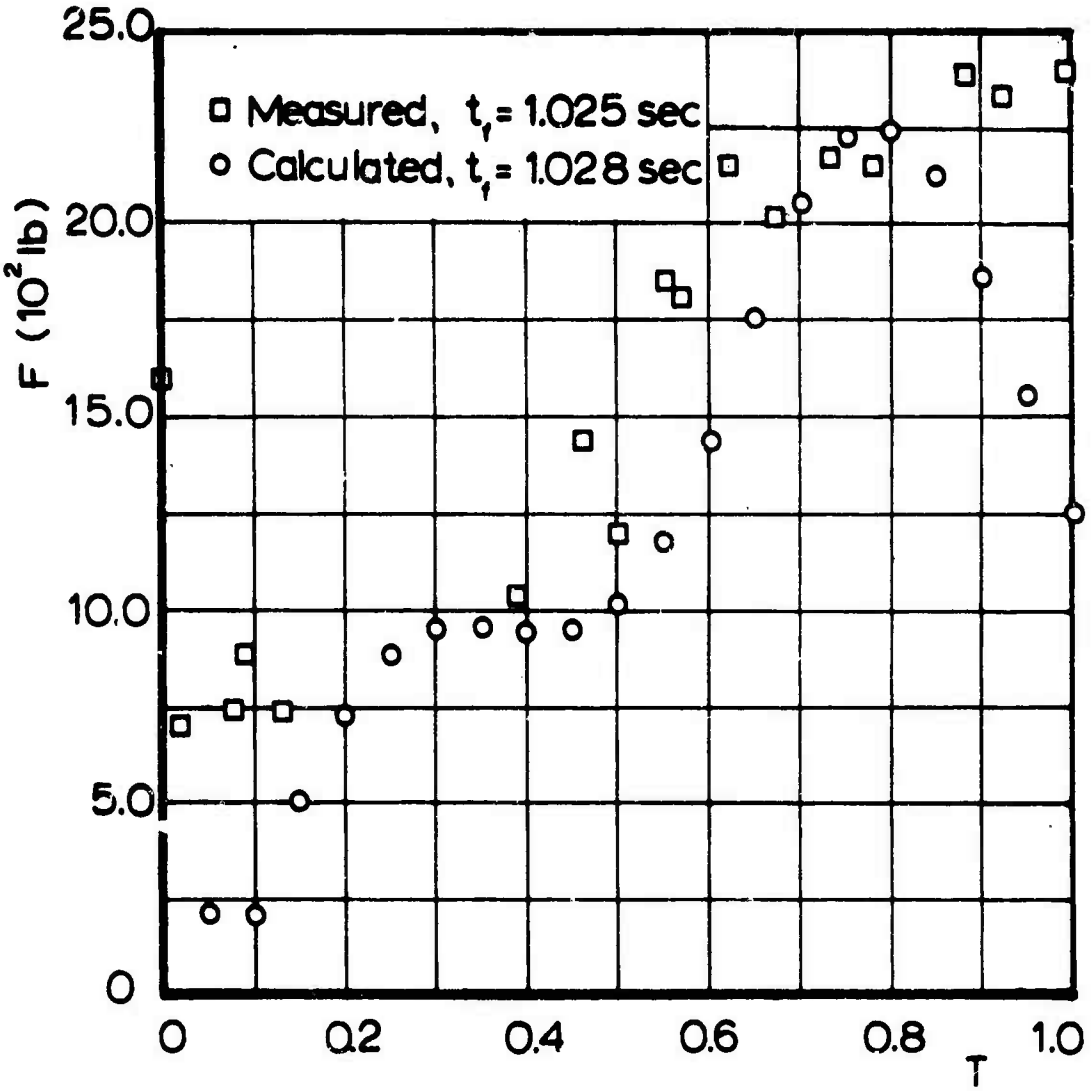

Fig 12 Calculated and Measured Force - Time Histories for a 28 ft Parachute, Test 1, v_s = 225 ft/sec, W_1 = 203 lb

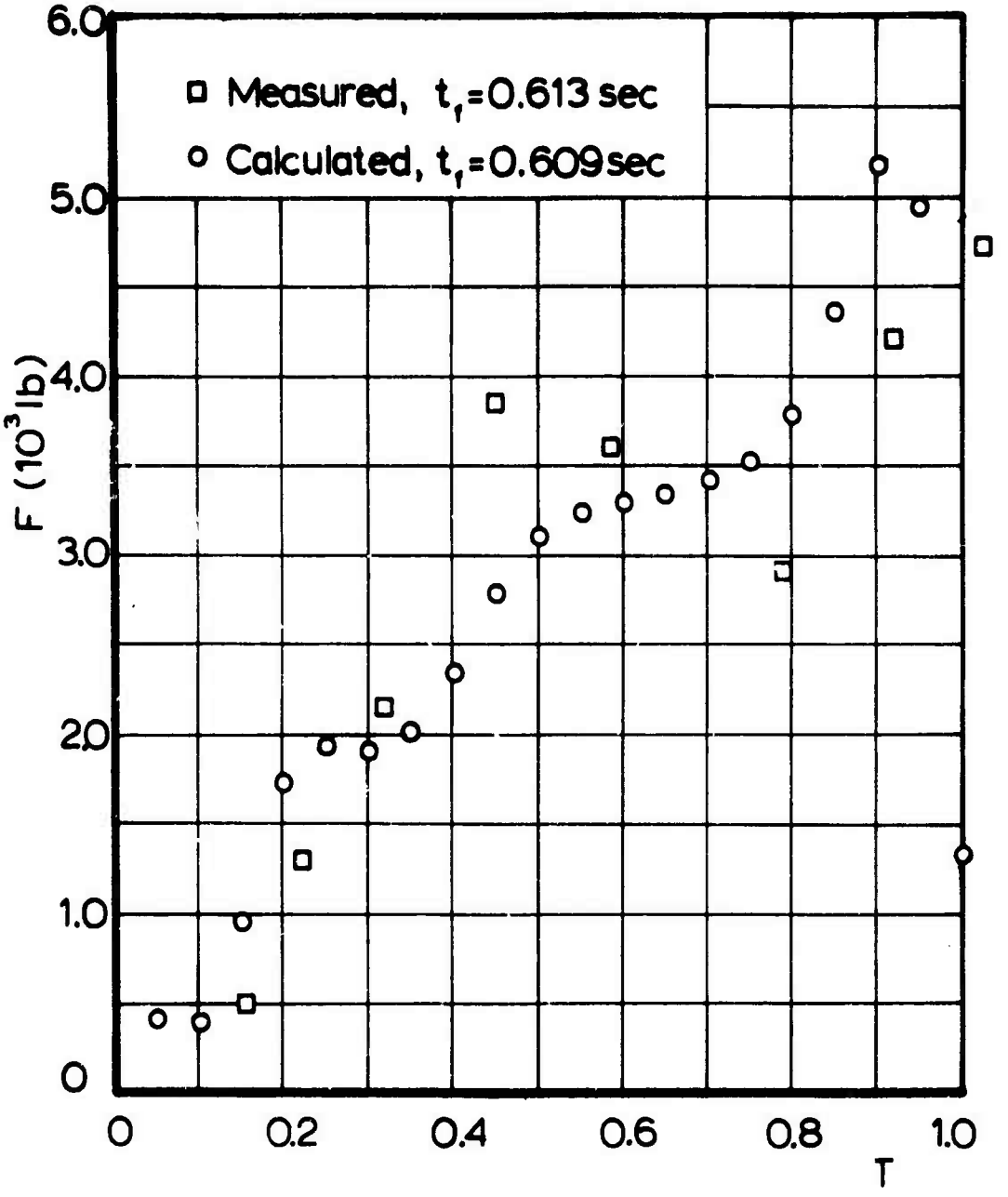

Fig 13 Calculated and Measured Force-Time Histories for a 28 ft Parachute, Test 9, v_s=306 ft/sec, W_L= 220 lb

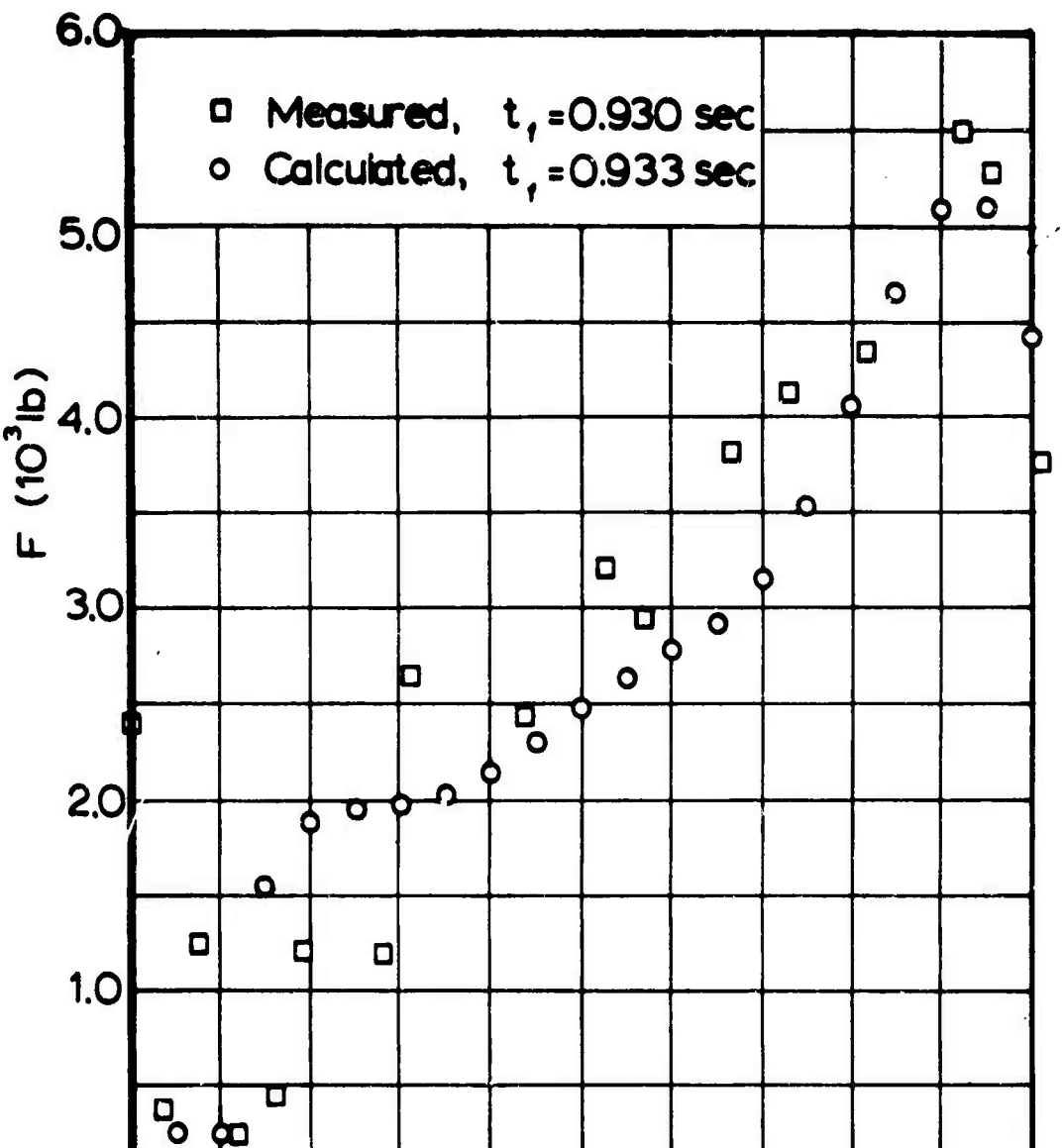

Fig 14 Measured and Calculated Force - Time Histories for a 28 ft Parachute, Test 44, v_s=255 ft/sec, W_s= 439 lb

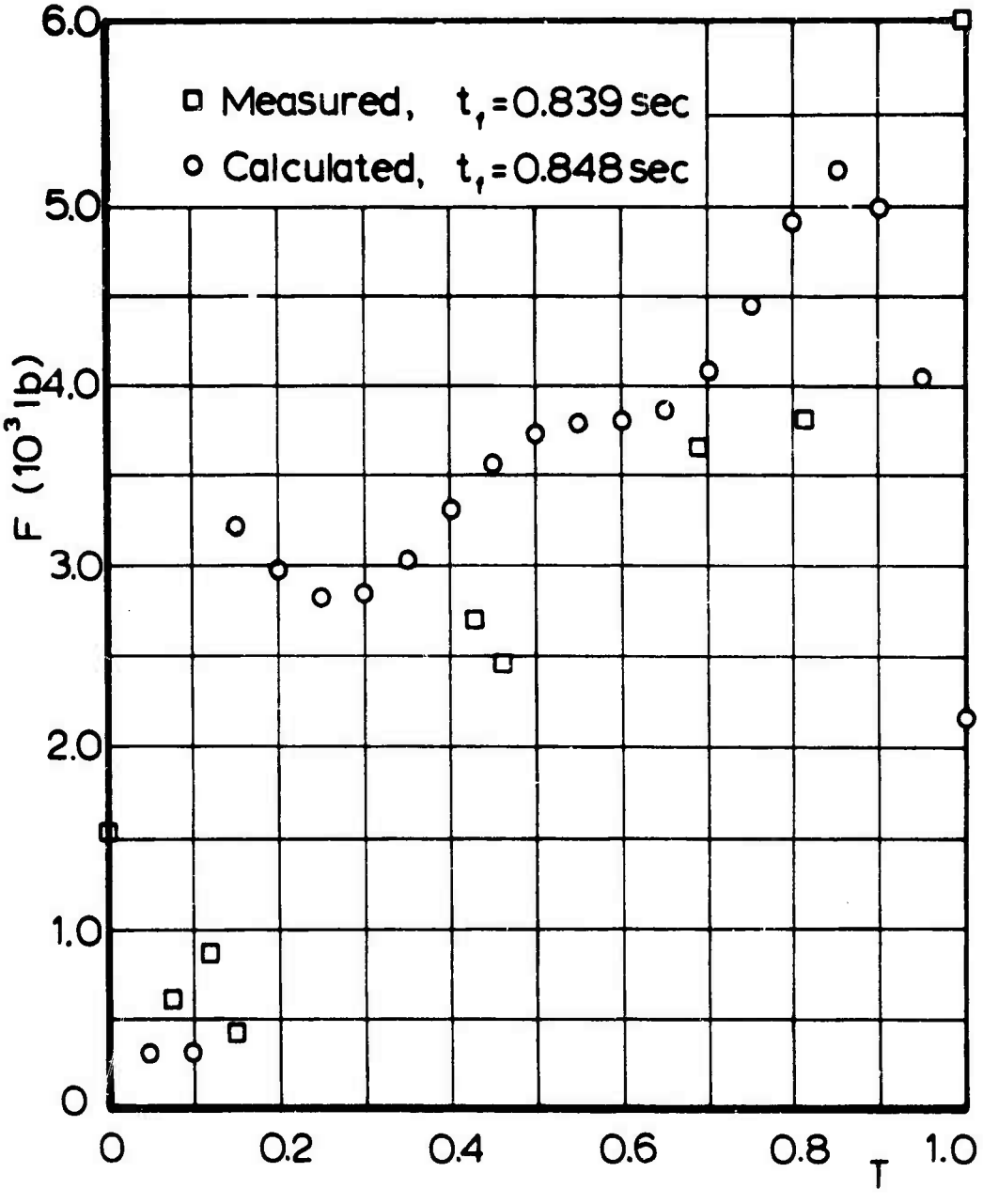

Fig 15 Calculated and Measured Force-Time Histories for a 28 ft Parachute, Test 39, v_s = 272 ft/sec, W_s = 439 lb

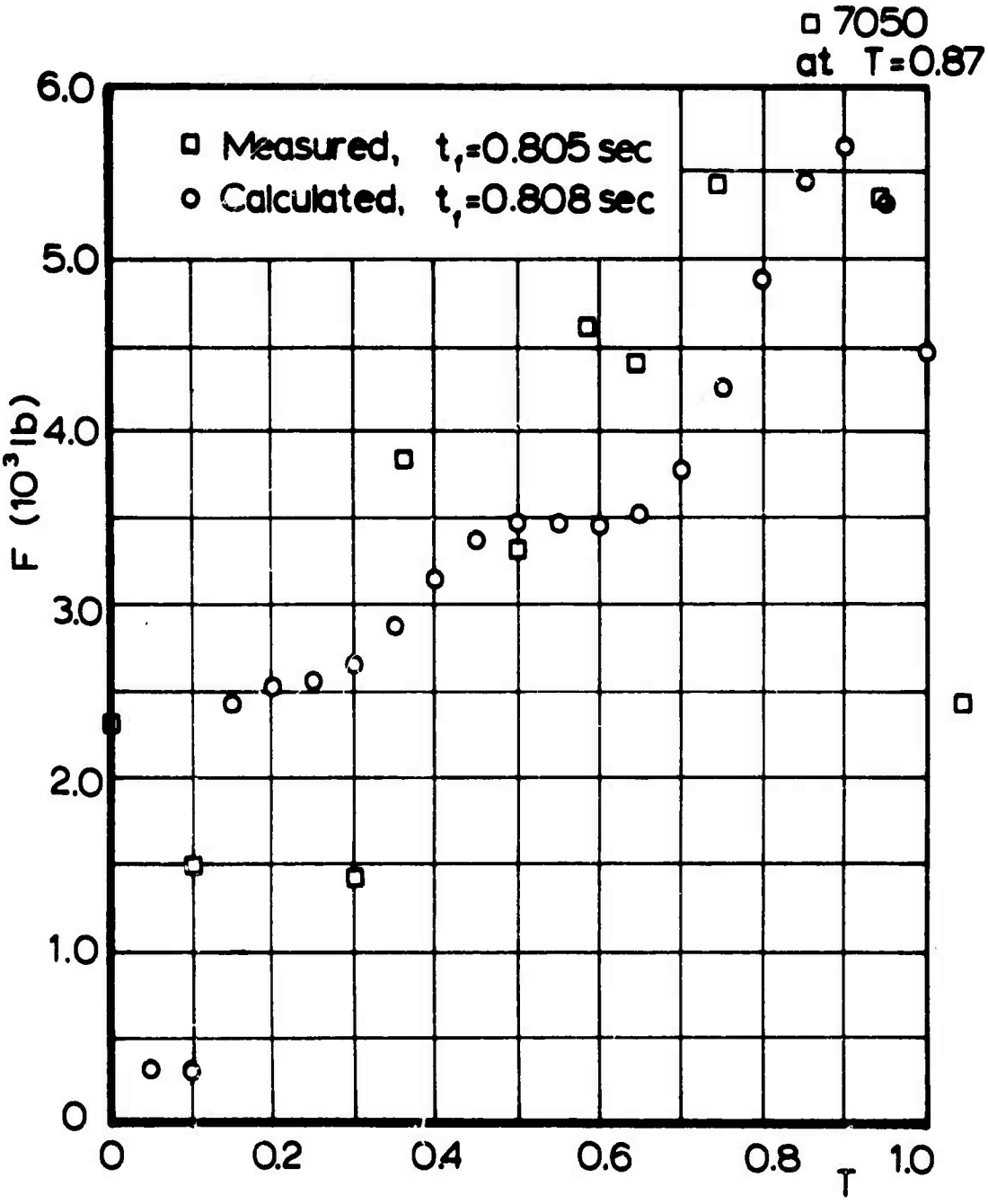

Fig 16 Calculated and Measured Force-Time Histories for a 28 ft Parachute, Test 43, v_s=275 ft/sec, W_L=439 lb

In these individual test cases, the calculations follow the general trend of the measured force-time relationships quite well, although in cases the magnitudes of calculated and measured maximum forces are somewhat different. The general conclusions that can be drawn from Figs 9 through 16, however, support the validity of the calculation method. More evaluation of carefully recorded field tests and more comparison is necessary before broader conclusions can be drawn. But the results show the best general force-time agreement for solid cloth parachutes that the authors are aware of. Maximum force calculations agreeing to a certain extent with measured maximum forces have been accomplished before; the advancement appears to be the accomplishment of matching force-time histories. A somewhat similar result for ribbon parachutes was achieved just recently by McVey and Wolf (Ref 26) who based their method on the same equation of motion and the momentum equation of finite sections of the parachute canopy. Their numerical input is based on a ratio of radial force to pressure drag coefficient C_r/C_D as function of geometric porosity λ_G.

The presented calculation method is based on the fundamental equations of motion and continuity. As empirical inputs one needs area- and inflow-time functions. Ideally one should have one set of functions which are suitable for all applications of parachutes of the same type over a large range of initial velocity and surface loading. An attempt to achieve this goal is described in the next chapter. The limited amount of complete experimental data available was a disadvantage. For further advancement of this method more evaluation of test records is needed; first for the establishment of good averages of parachute performance characteristics, and secondly for the extraction of area and inflow velocity time functions. The specific test information needed are the data for snatch velocity, force-time histories, and area-time histories.

IV. INFLATION ANALYSIS OF LARGE PARACHUTES

In the preceding chapter force-time histories were calculated for 3 ft and 28 ft solid cloth parachutes for which area-time relationships and filling times were available from wind tunnel or field tests. When these area-time curves and the related filling times were introduced into the general theory, the results were very good as shown in Figs 9 through 16.

The ultimate goal, however, was the establishment of unique dimensionless time histories of area and inflow functions which would provide inflation data valid for a wide variety of small and large parachutes, different surface loadings and initial velocities. Unfortunately, area-time histories of parachutes 64 ft or 100 ft in diameter were not available when this study was undertaken. Therefore, a number of 64 ft or 100 ft examples were calculated using area-time and inflow-time functions from tests with available experimental data. The general results are shown in Table I, and Table II indicates the combinations of numerical inputs. All force and velocity data related to 64 ft and 100 ft parachutes were obtained from Ref 27.

It can be seen that in a number of cases an individual set of area and inflow functions also covers cases with different functional conditions. For example, combinations 1, 4, 6, and 11 fit maximum opening forces of 3 ft as well as 64 ft and 100 ft parachutes. The term "fit" is applied when the deviation of the maximum measured and calculated forces is less than or equal to $\pm$ 10% of the measured maximum force.

The maximum measured forces of the 64 ft G-12D and 100 ft G-11A parachutes, as shown in Table I, are average

TABLE I PERCENT DEVIATION FROM MEASURED MAXIMUM FORCES, F_{max}, FOR VARIOUS AREA-TIME AND INFLOW-TIME FUNCTIONS

COMBINATION	CONFIG	3 ft MODEL PARACHUTE W_s = 0.5 lb			28 ft PARACHUTE W_s = 200 lb		28 ft PARACHUTE W_s = 440 lb			64 ft PARACHUTE W_s = 2200 lb		100 ft PARACHUTE 4550 lb	100 ft PARACHUTE 5410 lb
	V_s (ft/sec)	50	70	85	225	306	255	272	275	205*	240*	184*	156*
	F_{max} (lb)	6.5*	9.3*	16.9*	2400	4720	5490	5900	7050	6356*	7086*	9283*	8285*
1		-3	16	-11	-23	-25	93	106	72	-4	8	1	16
2		15	1	-22	-5	-9	70	81	51	17	17	-12	26
3		18	42	10	11	11	142	158	116	29	28	-8	34
4		0	20	-8	-17	-18	100	114	79	1	10	2	17
5		-40	-35	-52	-50	-56	-5	2	-17	19	-7	-9	-4
6		-4	12	-15	-36	-39	78	90	58	-8	3	-20	10
7		-40	-37	-54	-53	-59	-11	-5	-23	-28	-24	-33	-8
8		-23	-14	-36	-45	-50	29	39	14	-19	-11	-27	1
9		21	-9	-31	-30	-35	43	53	26	0	12	-14	-1
10		-12	5	-19	-16	-21	77	89	57	22	40	7	16
11		17	39	7	-22	-24	128	144	103	1	17	-2	17

Indicates Values ≤ ± 10% * Averaged Values

TABLE II AREA AND INFLOW FUNCTION DESCRIPTIONS FOR COMBINATIONS SHOWN IN TABLE I

CALC	AREA CURVE	INFLOW FUNCTION			
		D_o (ft)	W_s (lb)	v_s (ft/sec)	t_f (sec)
1	Measured - Test 44 (28 ft, 440 lb, 255 ft/sec, t_f = 0.93 sec)	28	203	255	0.92
2	Measured - Test 1 (28 ft, 200 lb, 225 ft/sec, t_f = 1.025 sec)	28	203	225	1.025
3	Measured - Test 9 (28 ft, 200 lb, 306 ft/sec, t_f = 0.613 sec)	28	220	306	0.613
4	Measured - Test 44 (28 ft, 440 lb, 255 ft/sec, t_f = 0.93 sec)	28	203	225	0.93
5	Measured - Test 44 (28 ft, 440 lb, 255 ft/sec, t_f = 0.93 sec)	28	439	255	0.93
6	Wind Tunnel Average - Model Parachute (3 ft, 0.5 lb, 50 ft/sec, t_f = 0.344 sec)	3	0.5	70	0.21
7	Wind Tunnel Average - Model Parachute (3 ft, 0.5 lb, 50 ft/sec, t_f = 0.344 sec)	3	0.5	70	0.344
8	Wind Tunnel Average - Model Parachute (3 ft, 0.5 lb, 50 ft/sec, t_f = 0.344 sec)	3	0.5	50	0.344
9	Wind Tunnel Average - Model Parachute (3 ft, 0.5 lb, 70 ft/sec, t_f = 0.21 sec)	3	0.5	70	0.21
10	Wind Tunnel Average - Model Parachute (3 ft, 0.5 lb, 85 ft/sec, t_f = 0.14 sec)	3	0.5	85	0.14
11	Empirical Function	64	2200	205	2.94

values of field tests (Ref 27) for which merely a few examples were available. The averaging process for the 64 ft parachute is described in the Appendix, and the results of this averaging process are shown in Fig 17. The maximum forces for the 100 ft parachute are based on averages of three field tests with 4,550 lb weight and two field tests with 5,410 lb weight.

Tables I and II indicate under combination 11 the results when an empirical set of area and inflow functions is used. This set was established after a considerable number of test cases were calculated and some experience was gained on the way these two functions influence the final force-time history. The area-time and the related inflow velocity-time functions are shown in Figs 18 and 19 and closely resemble some of the natural functions extracted from individual experiments. Their significance is that they match very closely the force-time history as well as the maximum forces of the 64 ft parachute as shown in Figs 20 and 21.

Looking at Fig 21 one may get the impression that the fit is not so good for the higher velocity. However, in this case the reported filling times for v_s = 205 ft/sec and 240 ft/sec are 2.94 sec and 3.70 sec, respectively. According to the presented theory, at the higher velocity the filling time would be expected to be shorter. Since the opposite is reported, one may suspect that the drop test results have been affected by random performance factors which were not accounted for in the theory. This is supported by Fig 22, which indicates that two drop tests have suspiciously low opening forces. The filling times for these two tests were unusually long, which in an averaging process involving merely four tests raised the average filling time

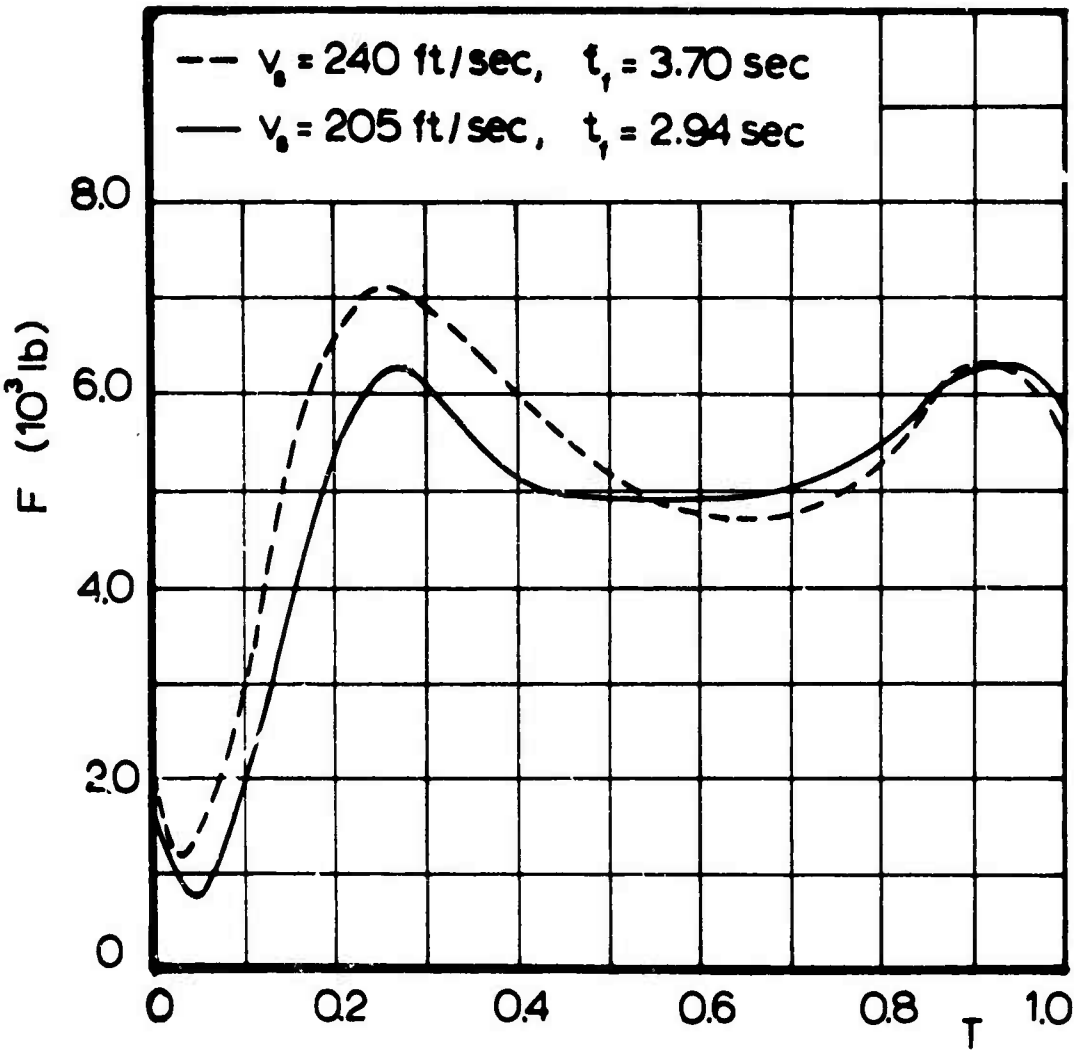

Fig 17 Averaged Measured Force - Time Histories for 64 ft, G-12D Parachute; W_L = 2200 lb

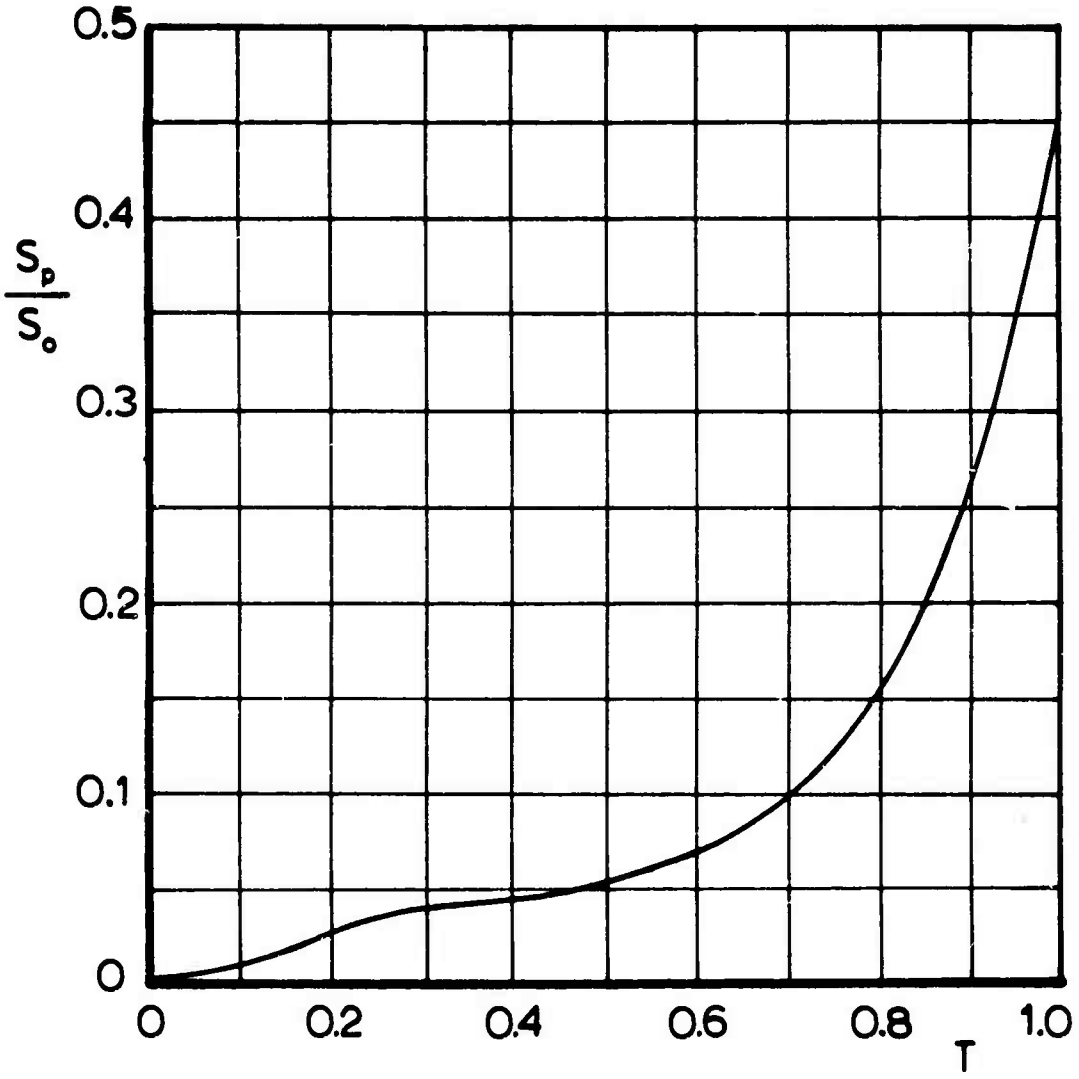

Fig 18 Empirical Projected Area - Time Function for Calculation of Opening Performance of Large Parachutes (Combination 11)

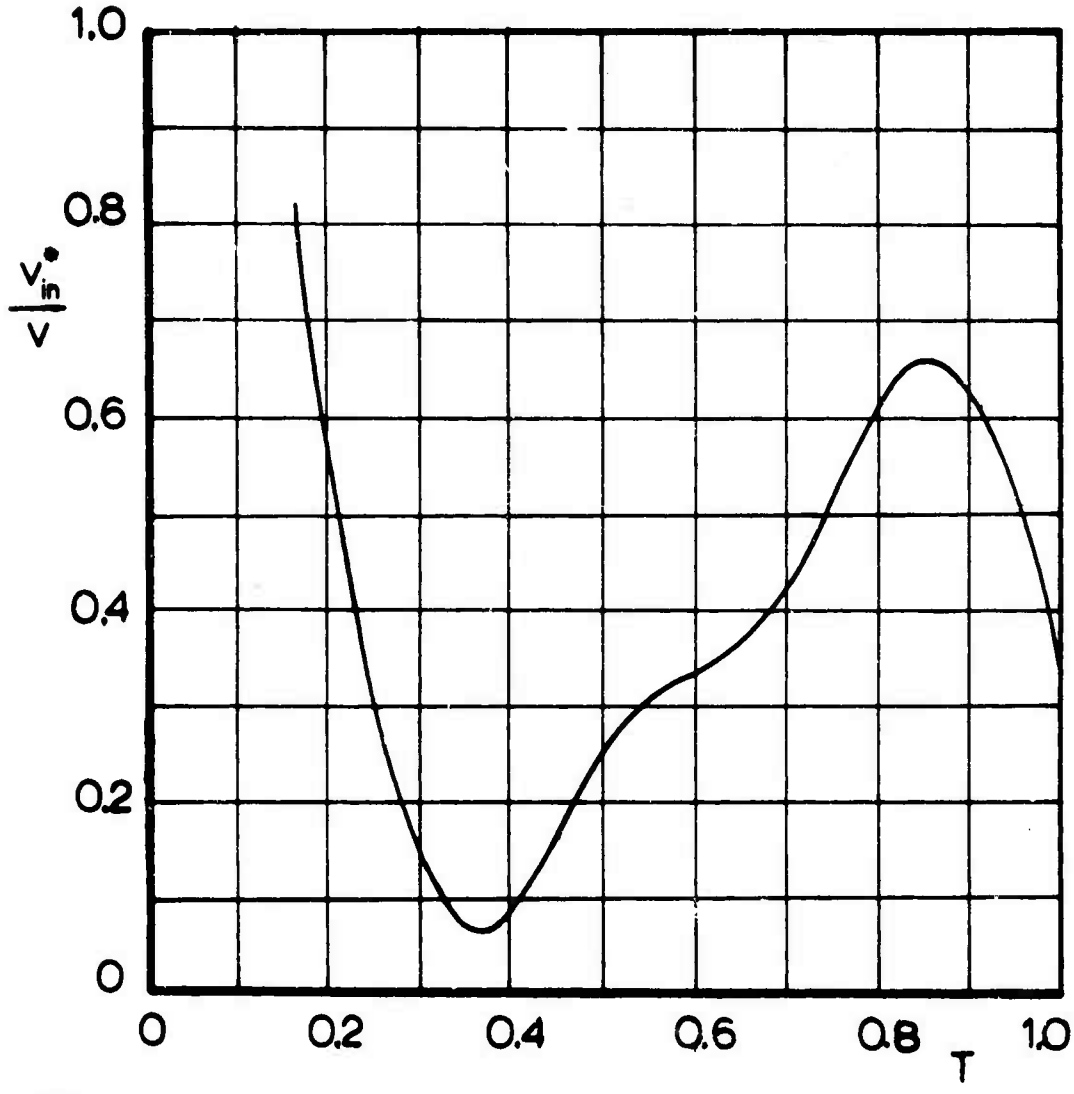

Fig 19 Empirical Inflow - Time Function for Calculation of Opening Performance of Large Parachutes (Combination 11)

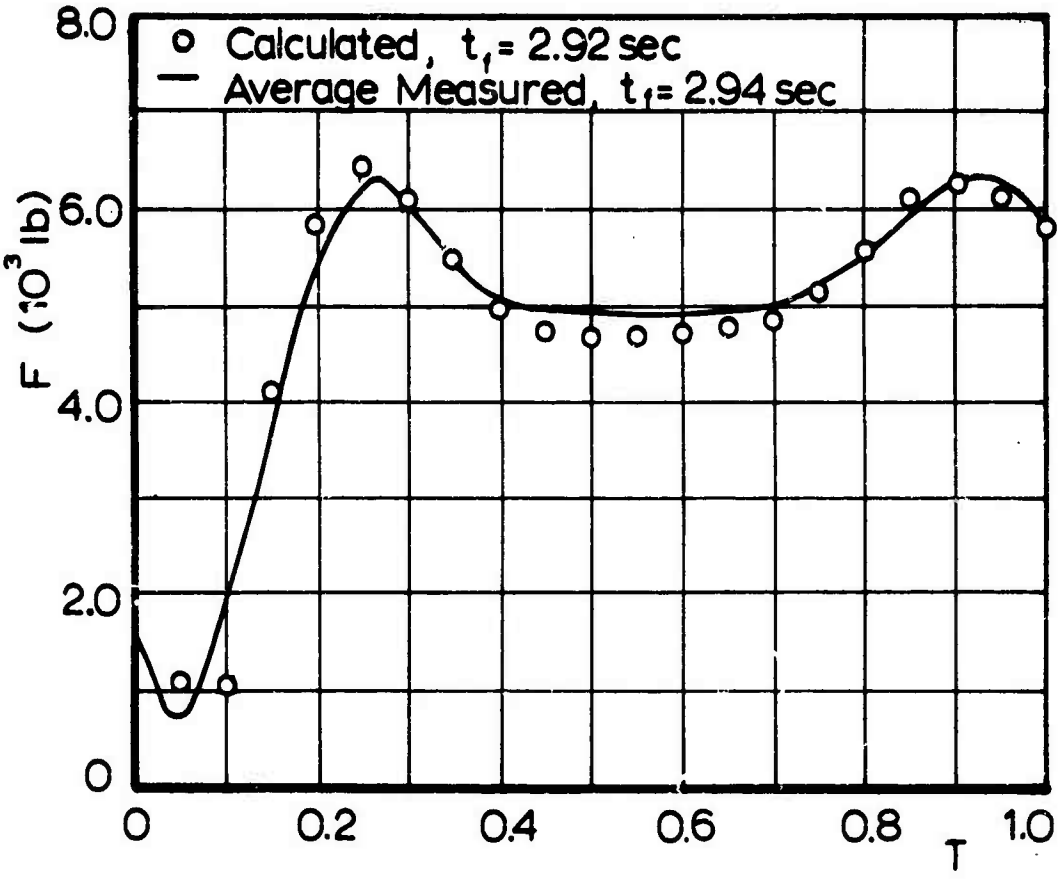

Fig 20 Calculated Force - Time History for 64 ft, G-12D Parachute Based on Empirical Inputs, Figs 18 and 19, Compared with Averaged Force - Time History ; W_L = 2200 lb, v_s = 205 ft/sec

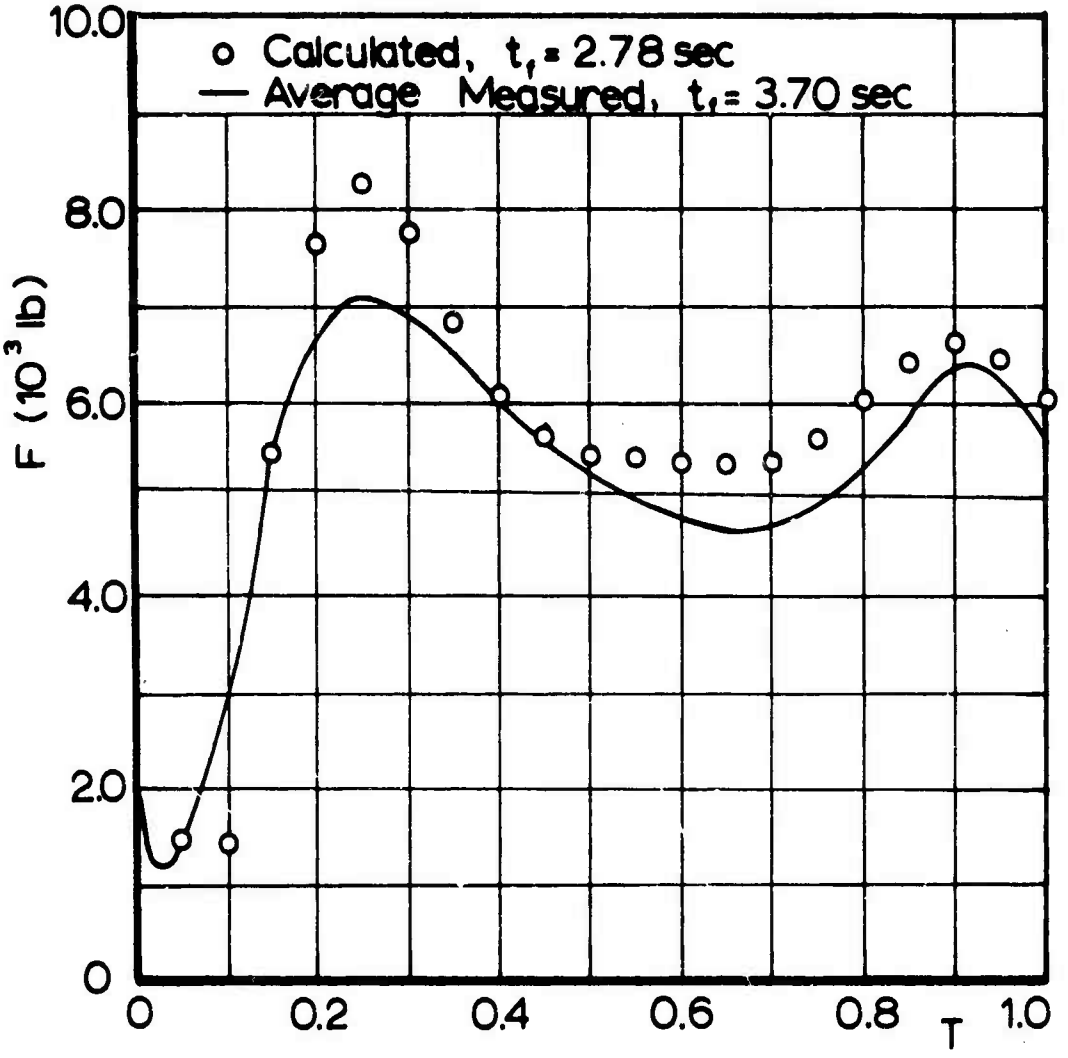

Fig 21 Calculated Force-Time History for 64 ft, G-12D Parachute Based on Empirical Inputs, Figs 18 and 19, Compared with Averaged Force-Time History; W_1 = 2200 lb, v_s = 240 ft/sec

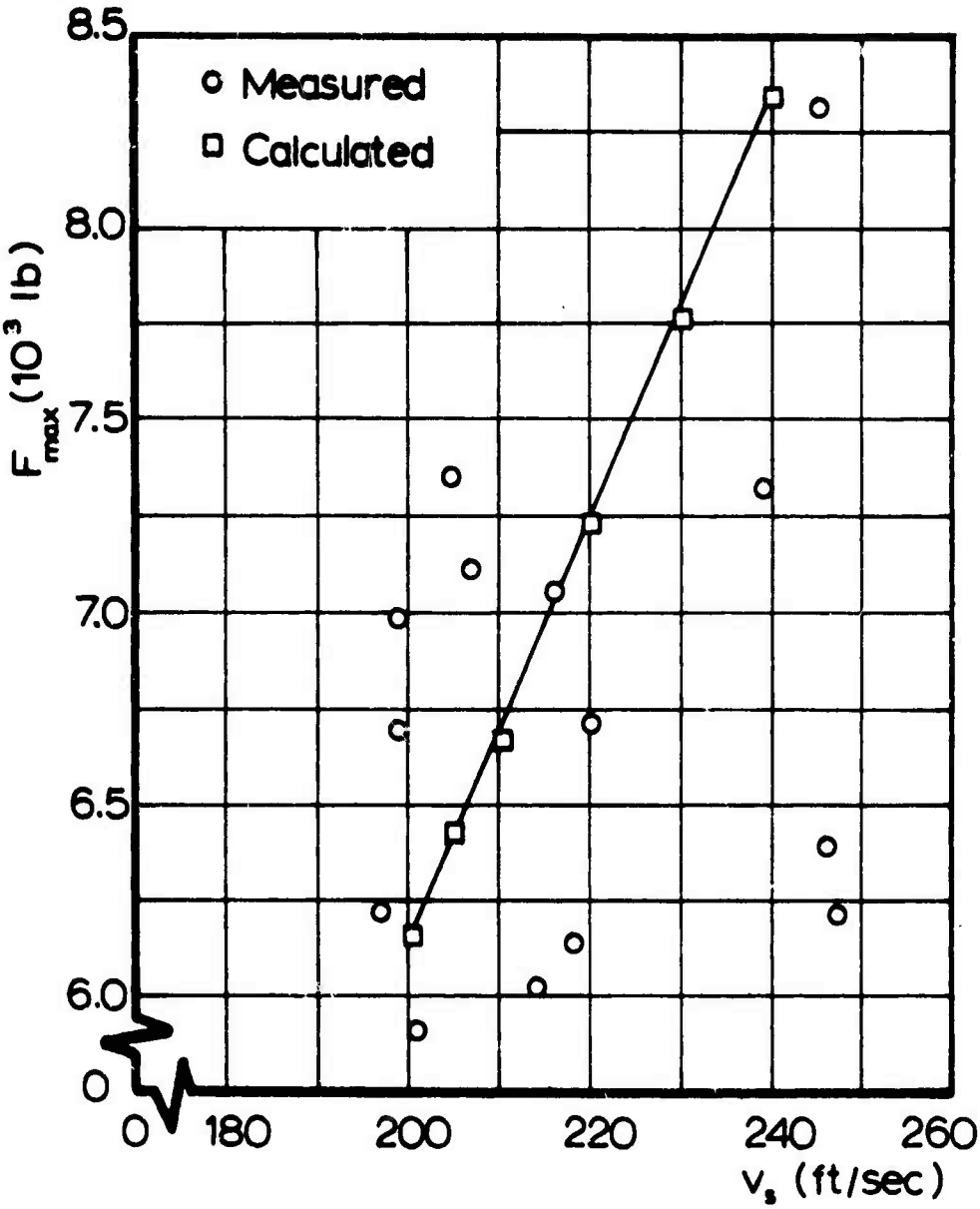

Fig 22 Calculated and Measured Maximum Forces for the 64 ft, G-12 D Parachute; W_1 = 2200 lb

and lowered the average force considerably.

In this case one might even conclude that the calculated maximum forces are a better indication of average maximum field test forces than the established average value. Figure 22 indicates otherwise a very good agreement between calculated and measured opening forces of the 64 ft parachute with 2200 lb suspended weight.

For the 100 ft parachute, G-11A, only the results of five applicable field tests were available, and these are reproduced as well as possible in Figs 23 through 27. It will also be noticed that the forces are plotted against real time. This was necessary since it was impossible to determine from field test recordings the points of T = 0 and T = 1. The figures indicate also that in all cases, the measured and calculated force-time histories show considerable differences, whereas the calculated and measured maximum forces agree quite well (Fig 28). The only exception is the test with lowest snatch velocity. However, the measured force for this velocity is suspiciously low as can be seen in Fig 28. Furthermore, the discrepancies between calculated and measured forces is probably enhanced, since it was impossible to establish a dimensionless time scale.

The calculations for the 100 ft parachute, shown in Figs 23 through 28, were carried out with the empirical combination No. 11, the same as used for the 64 ft parachute. In view of the small number of field tests and the agreement between calculated and measured maximum forces, the method described in the first part of this report and the numerical input No. 11 appear to be useful for the G-11A parachute as well as the G-12D parachute. Once more and better field test data become available, the case of the 64 ft and 100 ft parachutes should be reviewed in order to establish a more unique numerical input for large cargo parachutes.

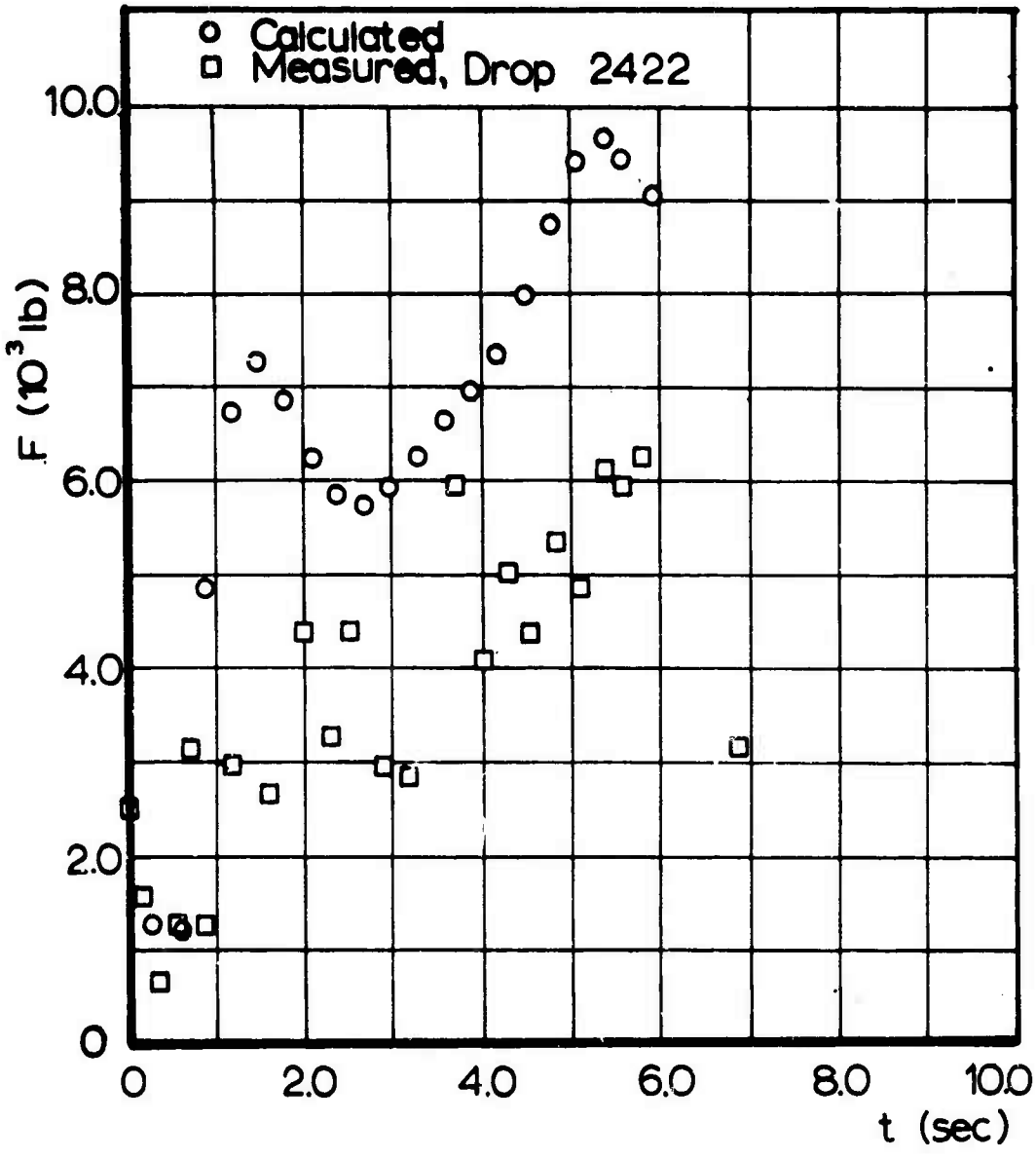

Fig 23 Calculated and Measured Force-Time Histories for 100 ft, G-11 A Parachute Based on Empirical Inputs, Figs 18 and 19; W_a = 5410 lb, v_s = 136 ft/sec

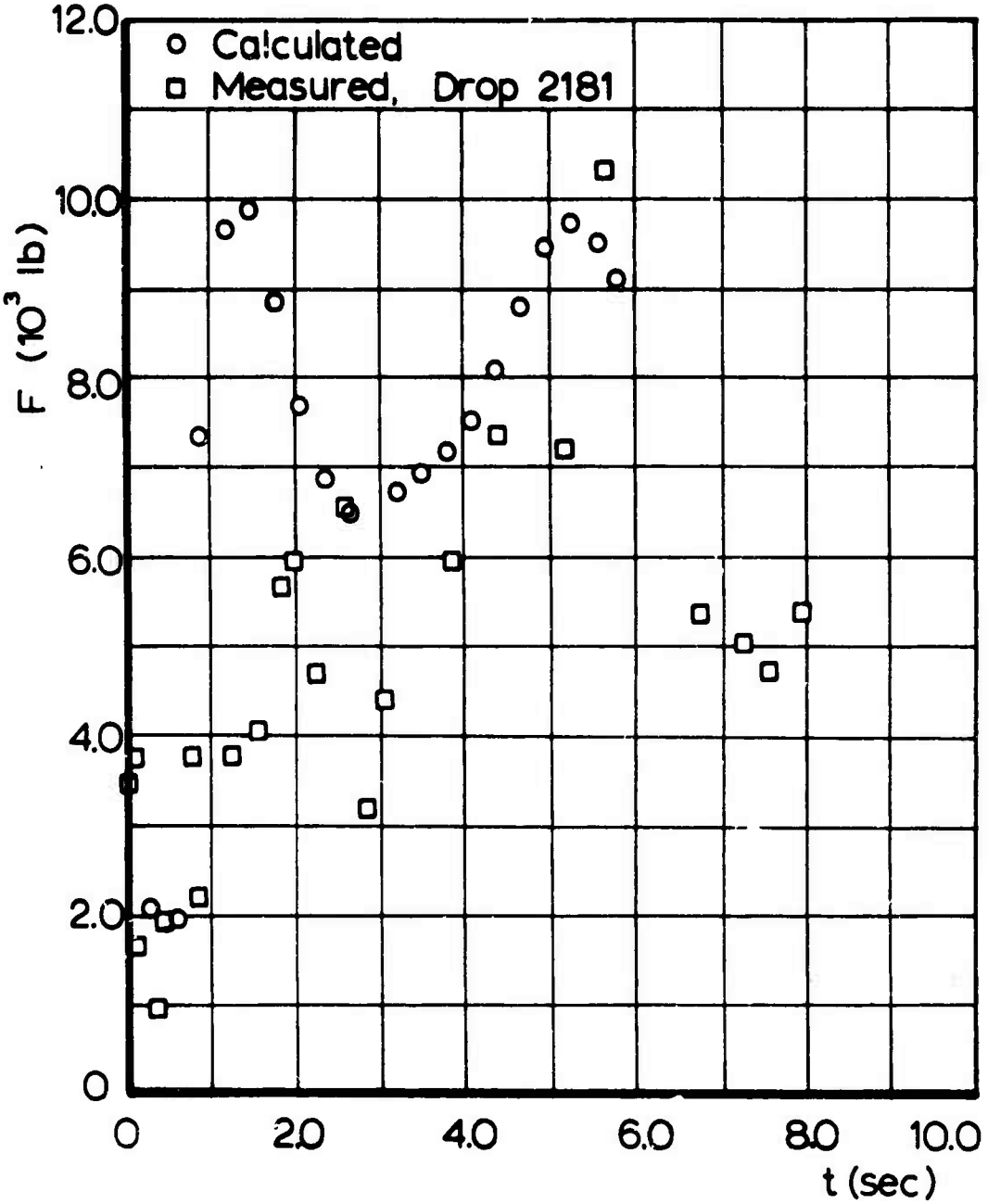

Fig 24 Calculated and Measured Force-Time Histories for 100 ft, G-11A Parachute Based on Empirical Inputs, Figs 18 and 19; $W_1 = 5410$ lb, $v_s = 177$ ft/sec

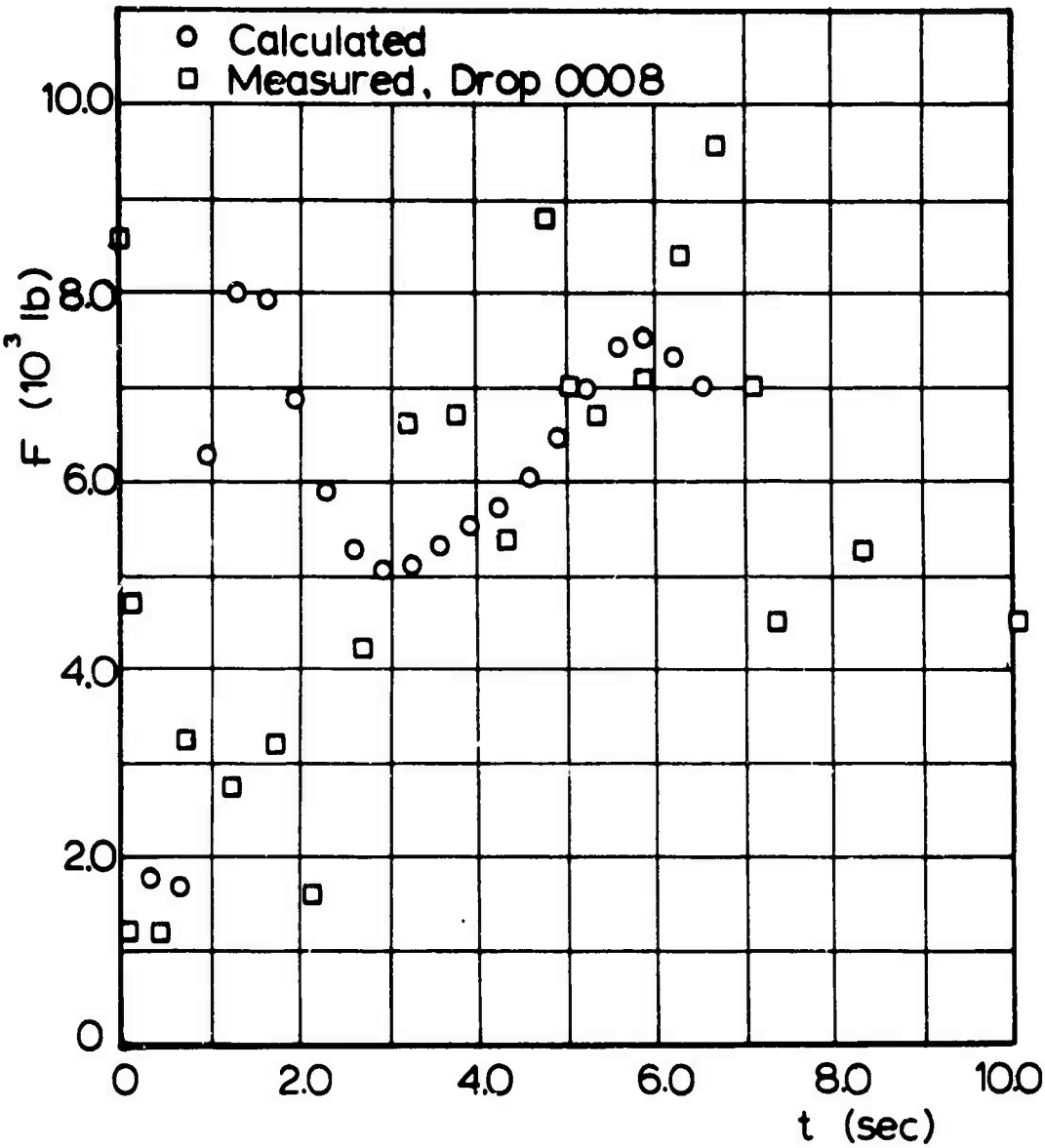

Fig 25 Calculated and Measured Force - Time Histories for 100 ft, G-11A Parachute Based on Empirical Inputs, Figs 18 and 19; W_1 = 4550 lb V_s = 168 ft/sec

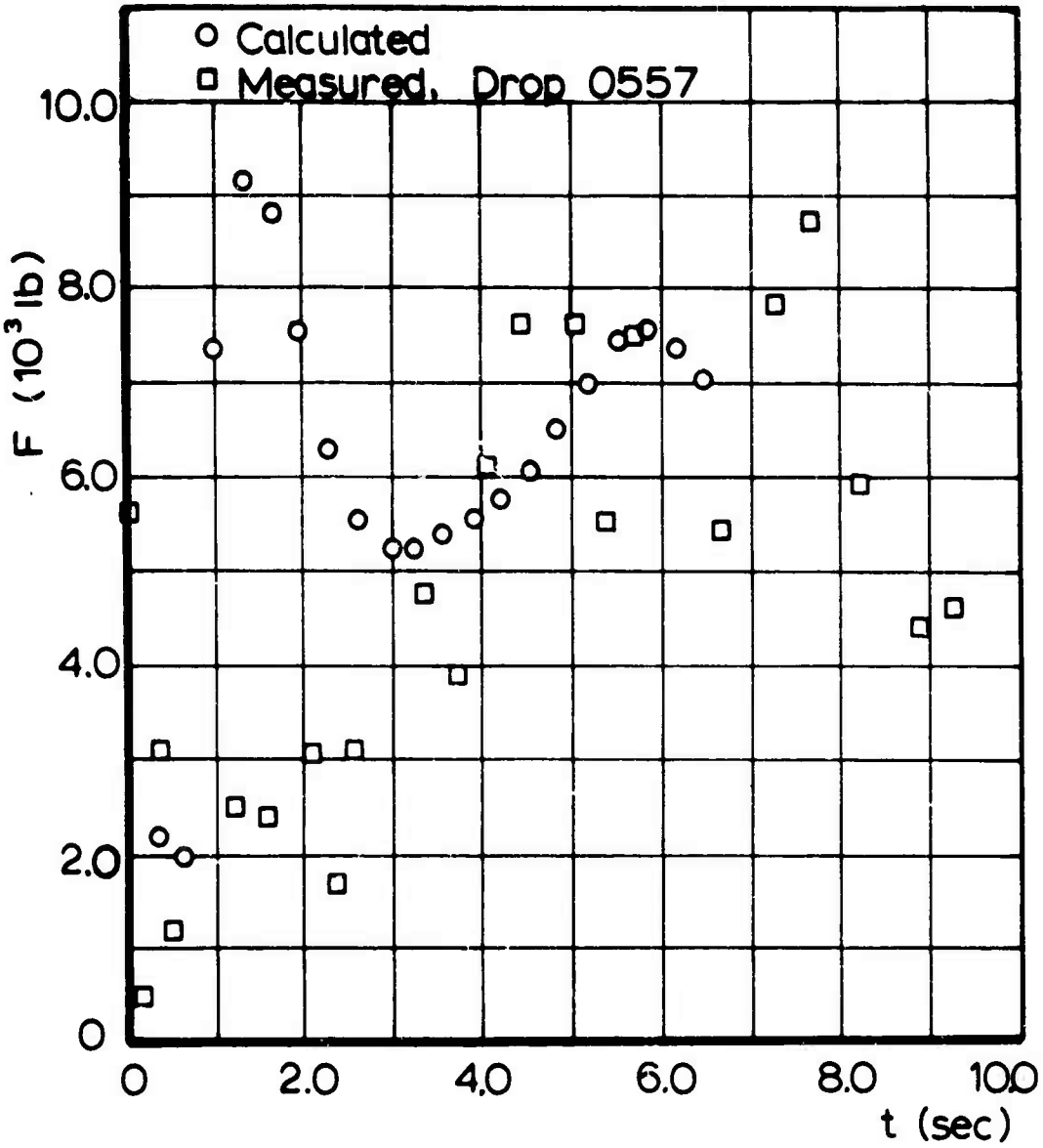

Fig 26 Calculated and Measured Force-Time Histories for 100 ft, G-11 A Parachute Based on Empirical Inputs, Figs 18 and 19 ; W_s = 4550 lb, v_s = 187 ft/sec

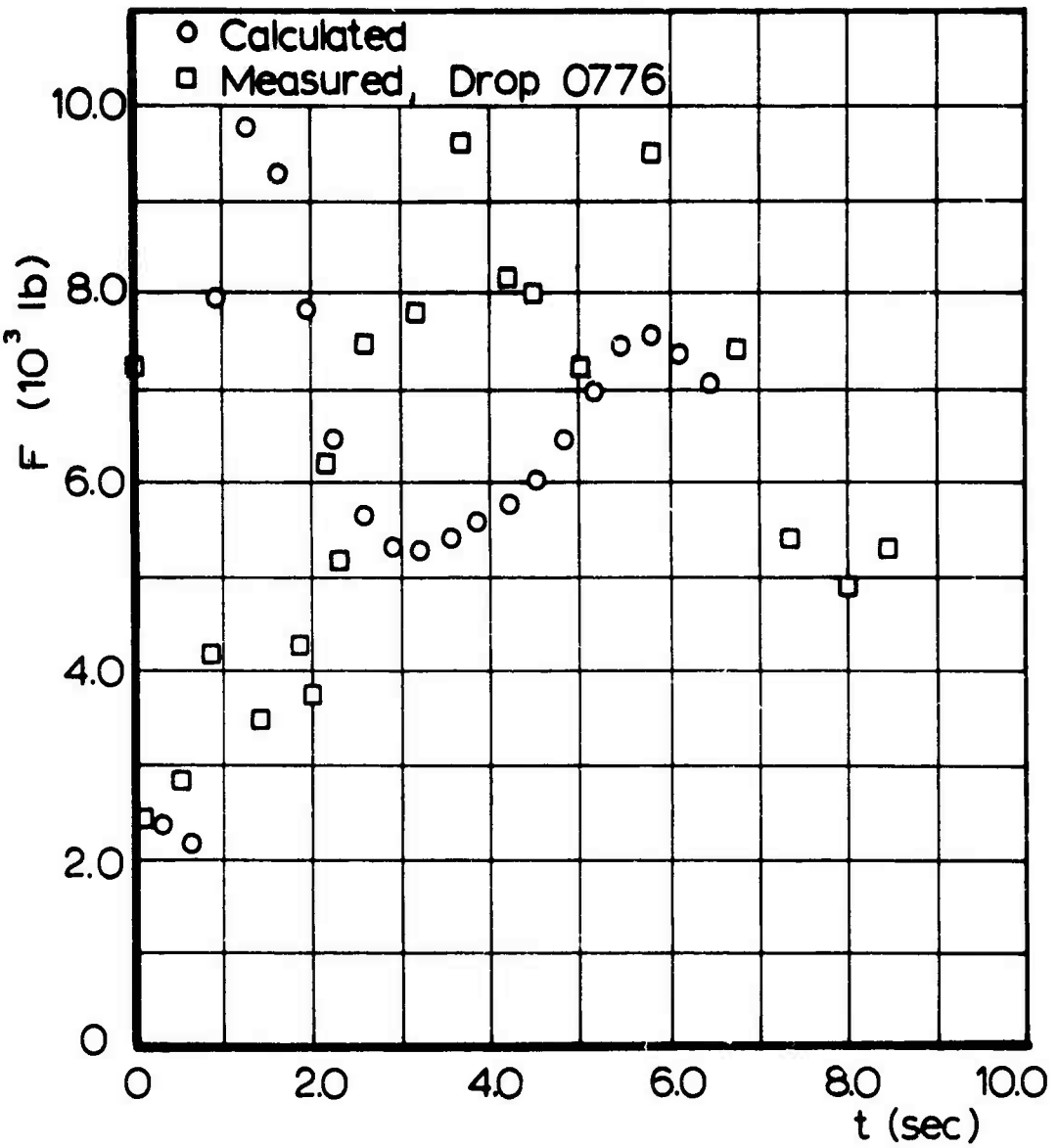

Fig 27 Calculated and Measured Force - Time Histories for 100 ft, G-11A Parachute Based on Empirical Inputs, Figs 18 and 19; W_t = 4550 lb, v_s = 197 ft/sec

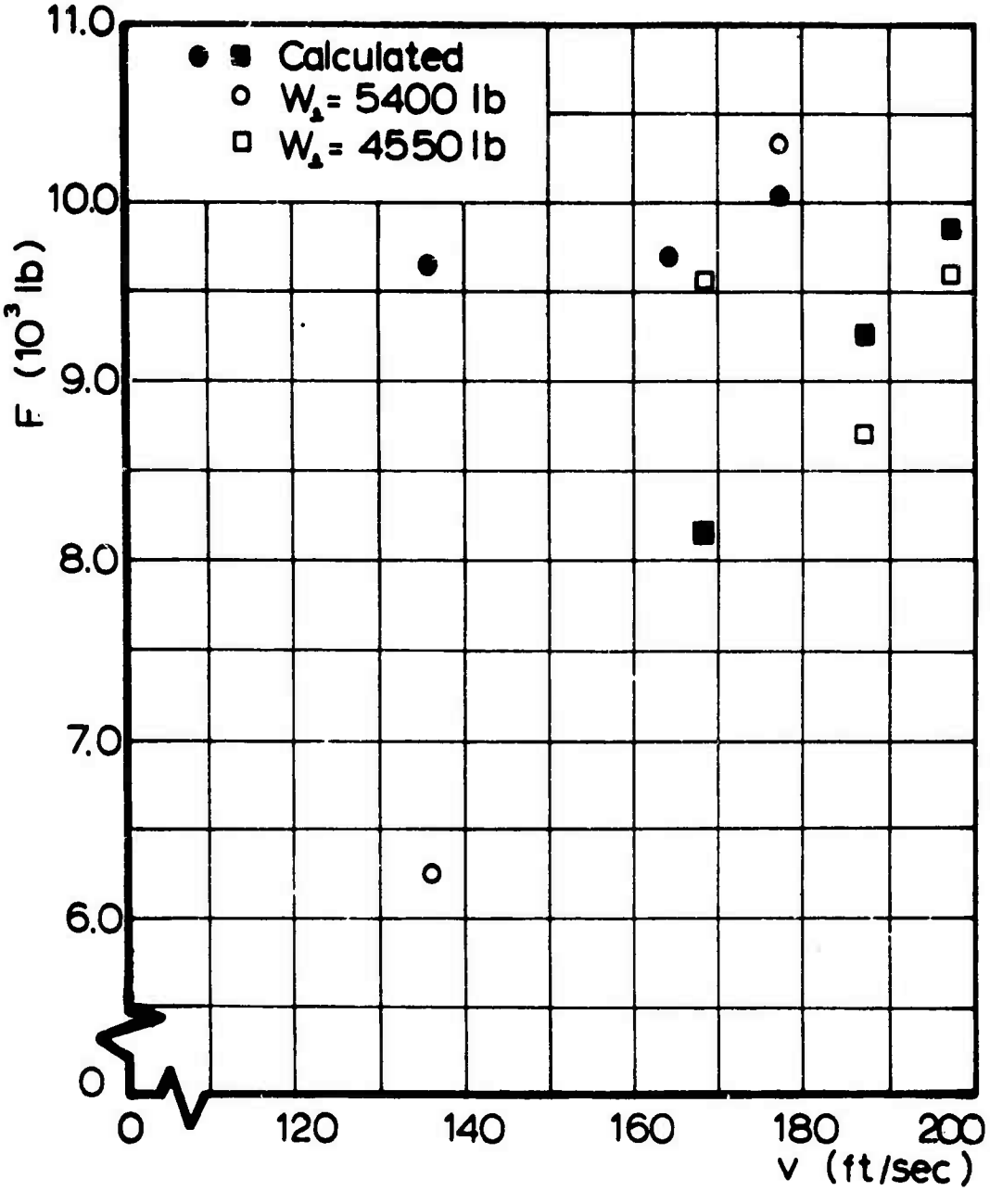

Fig 28 Calculated and Measured Maximum Forces for the 100 ft, G-11A Parachute

V. REVIEW OF THE NUMERICAL INPUTS

Throughout this study it was found that in many cases for which a reliable area-time history existed, the calculated and measured force-time history and the maximum forces agreed satisfactorily. This proves that the method of calculation is, in principle, correct.

The study did not provide a unique area-time history which covered all cases under consideration. However, several time functions of area and inflow velocity were established which provided good matches for certain parachute applications.

For example, the combination No. 11 appears to be very suitable for applications involving the 64 ft and 100 ft parachute with surface loadings (W/S_o) in the order of 0.58 to 0.69 lb/ft^2. Because of this significance, the coefficients for the area-time and inflow-time polynomial functions which were shown in Figs 18 and 19 are tabulated in Table III. These coefficients defined the polynomials used as the numerical inputs to the calculation procedure described previously. The polynomial fits with least mean square error when compared with the respective functions were selected by means of a computer subroutine. The order of the polynomial is determined by the computer up to a maximum of 10. It was found that allowing higher order curve fits did not significantly change results. It is very likely that carrying the coefficients out to the number of figures shown is not necessary, but in all calculations the coefficients were used as tabulated.

Other combinations of area-time and inflow-time functions also gave results that matched several test conditions. From Table I, the best of these were combinations Nos. 1,

TABLE III

COEFFICIENT OF T^n FOR POLYNOMIAL APPROXIMATIONS TO AREA AND INFLOW FUNCTIONS FOR COMBINATION 11 ; NUMERICAL INPUTS FOR COMPUTER CALCULATION

n	S_p / S_o	v_{in}^* / v
0	0.0	5.2738316591
1	0.2971001416	- 68.0062803176
2	- 6.5123855649	398.9198845511
3	73.2524253316	- 789.1636783155
4	- 377.1619626323	- 3727.8438477437
5	1048.4266537647	27891.6563064437
6	-1682.6596027555	- 78666.2022355702
7	1561.9500310581	121237.1222637268
8	- 778.5894164219	-107103.9511908507
9	161.4535189751	50971.3938078692
10	---------	- 10148.8700778727

4, 5, and 6, which are plotted in Figs 29 through 32. The polynomial coefficients of these functions are shown in Tables IV to VII. A selection of any one of these combinations would depend on the application, and Table I could be used as a guide.

Of all combinations examined, No. 4 comes the closest to being unique, considering maximum forces, force-time histories, and filling times. Plots of force vs dimensionless time derived using this combination for 3 ft, 28 ft, and 64 ft tests are shown in Figs 33 through 35. As shown in the figures the calculated and measured filling times did not always agree perfectly. The force-time fit in Fig 33 for the 3 ft model is excellent, and that in Fig 34 for the 28 ft test is not as good, but certainly an improvement over previous calculation methods.

Comparing Fig 35 and Fig 20 for the average of 64 ft G-12D parachute at a snatch velocity of 205 ft/sec points out that there is little difference in combinations Nos. 4 and 11. Combination No. 11 basically follows from combination No. 4 with the objective of better matching the force-time history of large parachutes.

Since combinations 4 and 11 are very similar, Figs 23 through 27 are, in principle, similar to the match of measured force-time histories and those calculated from combination No. 4.

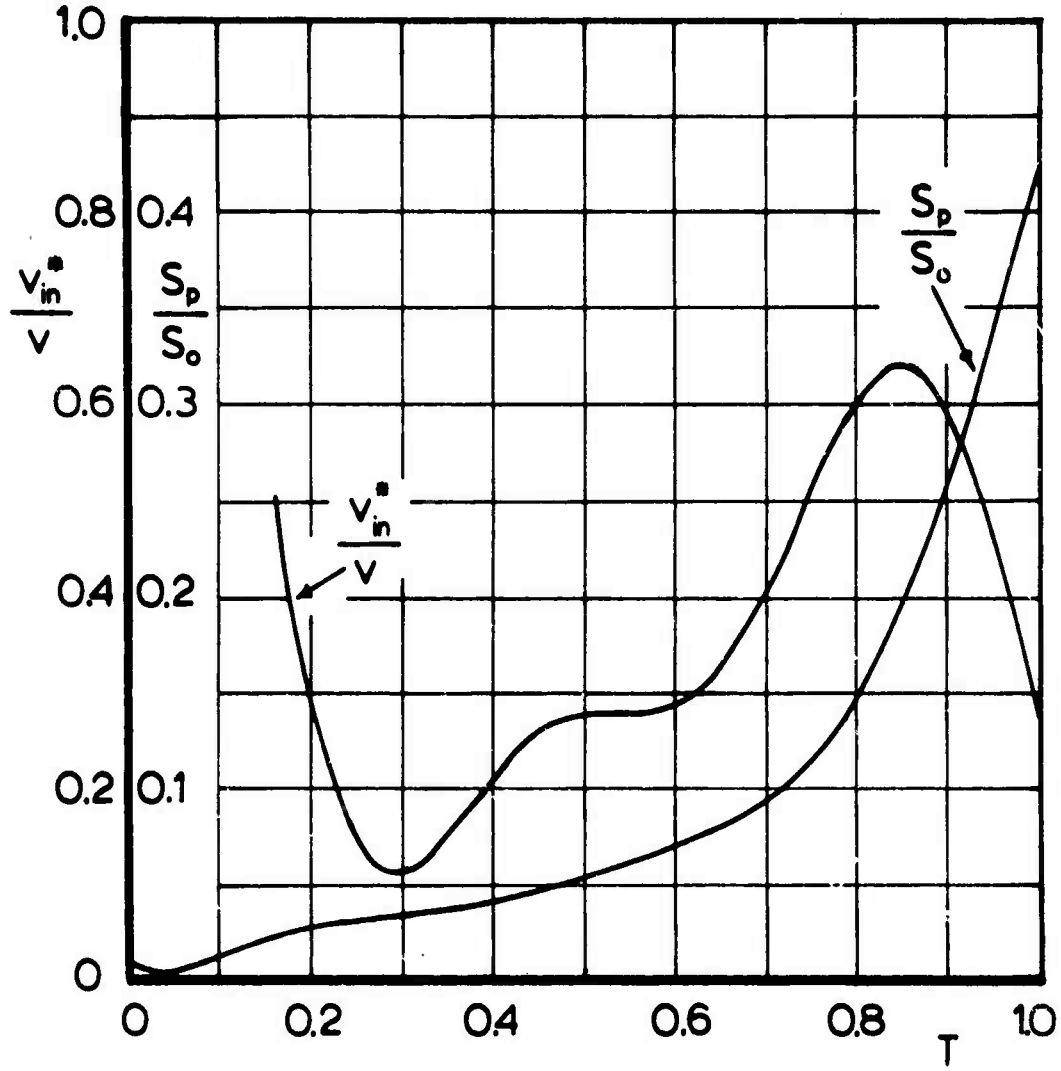

Fig 29 Area and Inflow Functions for Combination 1

TABLE IV

COEFFICIENT OF T^n FOR POLYNOMIAL APPROXIMATIONS TO AREA AND INFLOW FUNCTIONS FOR COMBINATION 1 ; NUMERICAL INPUTS FOR COMPUTER CALCULATION

n	S_p / S_o	v_{in}^* / v
0	0.0085739969	6.84209453
1	- 0.3142731955	- 123.8394952045
2	6.3387516302	1135.0720745963
3	- 37.0038652454	- 6430.731274966
4	104.764925497	23432.3178700899
5	-154.8224168382	-55290.2921097623
6	114.8199749927	84389.7972216229
7	- 33.3718099606	-82060.9779314171
8	--------	48718.4278991739
9	---------	-15967.8323568559
10	---------	2191.5147999854

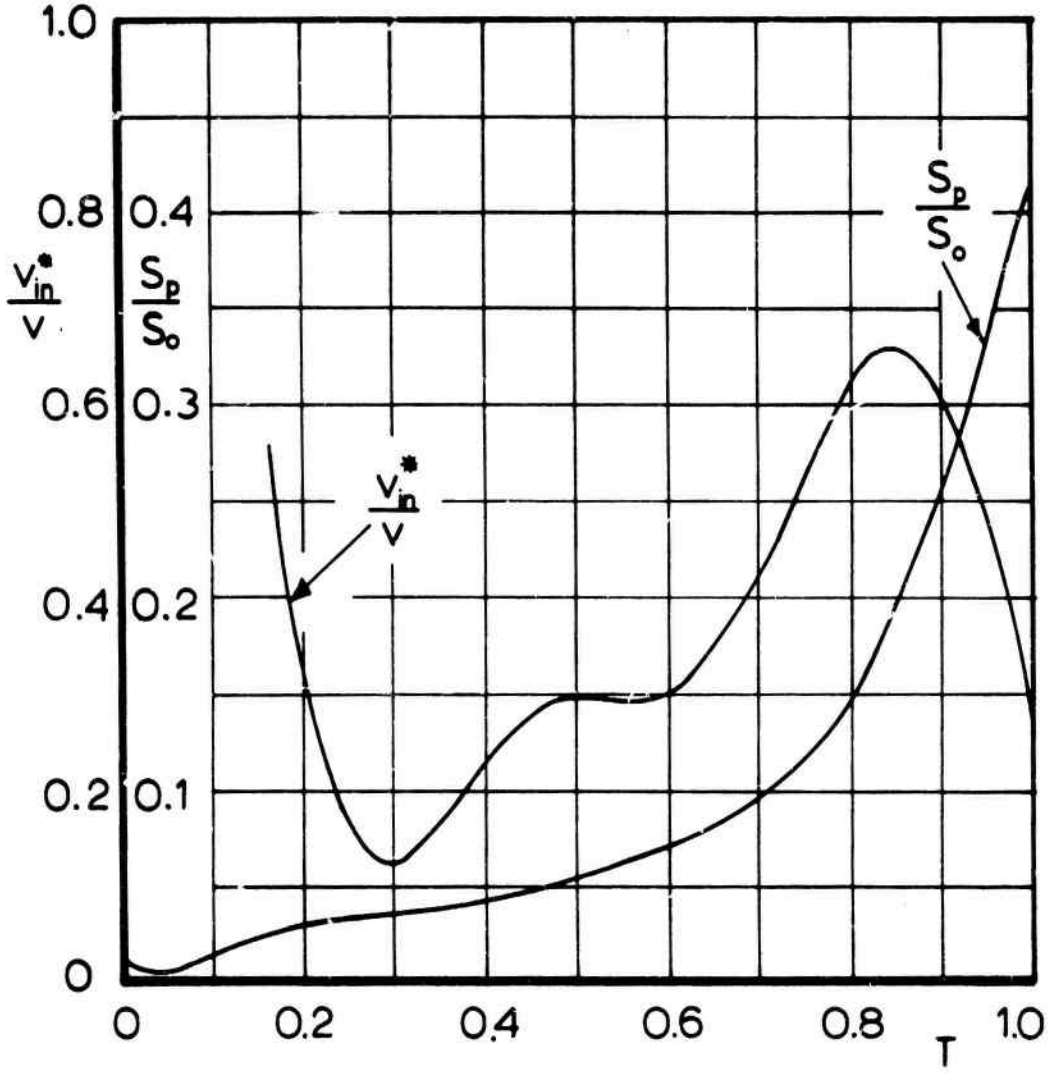

Fig 30 Area and Inflow Functions for Combination 4

TABLE V

COEFFICIENT OF T^n FOR POLYNOMIAL APPROXIMATIONS TO AREA AND INFLOW FUNCTIONS FOR COMBINATION 4 ; NUMERICAL INPUTS FOR COMPUTER CALCULATION

n	S_p / S_o	v_{in}^* / v
0	0.0085739969	7.6102494894
1	- 0.3142731955	- 137.8804577755
2	6.3387516302	1262.5925586515
3	- 37.0038652454	- 7164.1424886181
4	104.764925497	26219.421218405
5	-154.8224168382	-62319.421952C669
6	114.8199749927	96114.9720397033
7	-33.3718099606	-94799.4705938455
8	--------	57370.0070345635
9	--------	-19300.8977513466
10	--------	2747.4930266612

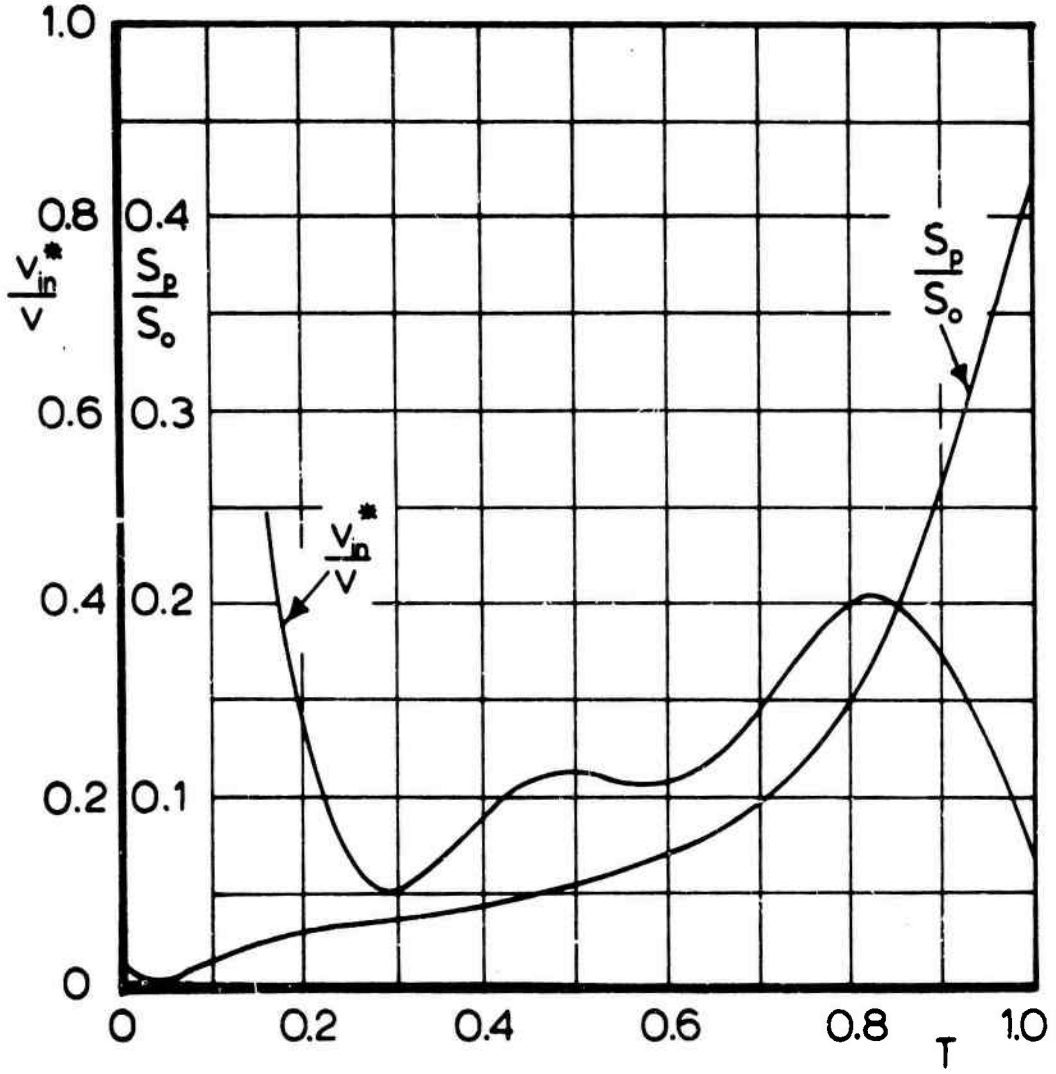

Fig 31 Area and Inflow Functions for Combination 5

TABLE VI

COEFFICIENT OF T^n FOR POLYNOMIAL APPROXIMATIONS TO AREA AND INFLOW FUNCTIONS FOR COMBINATION 5 ; NUMERICAL INPUTS FOR COMPUTER CALCULATION

n	S_p / S_o	V_{in}^* / V
0	0.0085739969	6.6577605215
1	- 0.3142731955	- 119.2167880803
2	6.3387516302	1081.9969705553
3	- 37.0038652454	- 6136.8437811568
4	104.764925497	22643.3875232526
5	-154.8224168382	-54643.8108733129
6	114.8199749927	86082.7160893832
7	- 33.3718099606	-87234.6065837992
8	--------	54590.095479002
9	--------	-19136.4518430873
10	--------	2866.2244175343

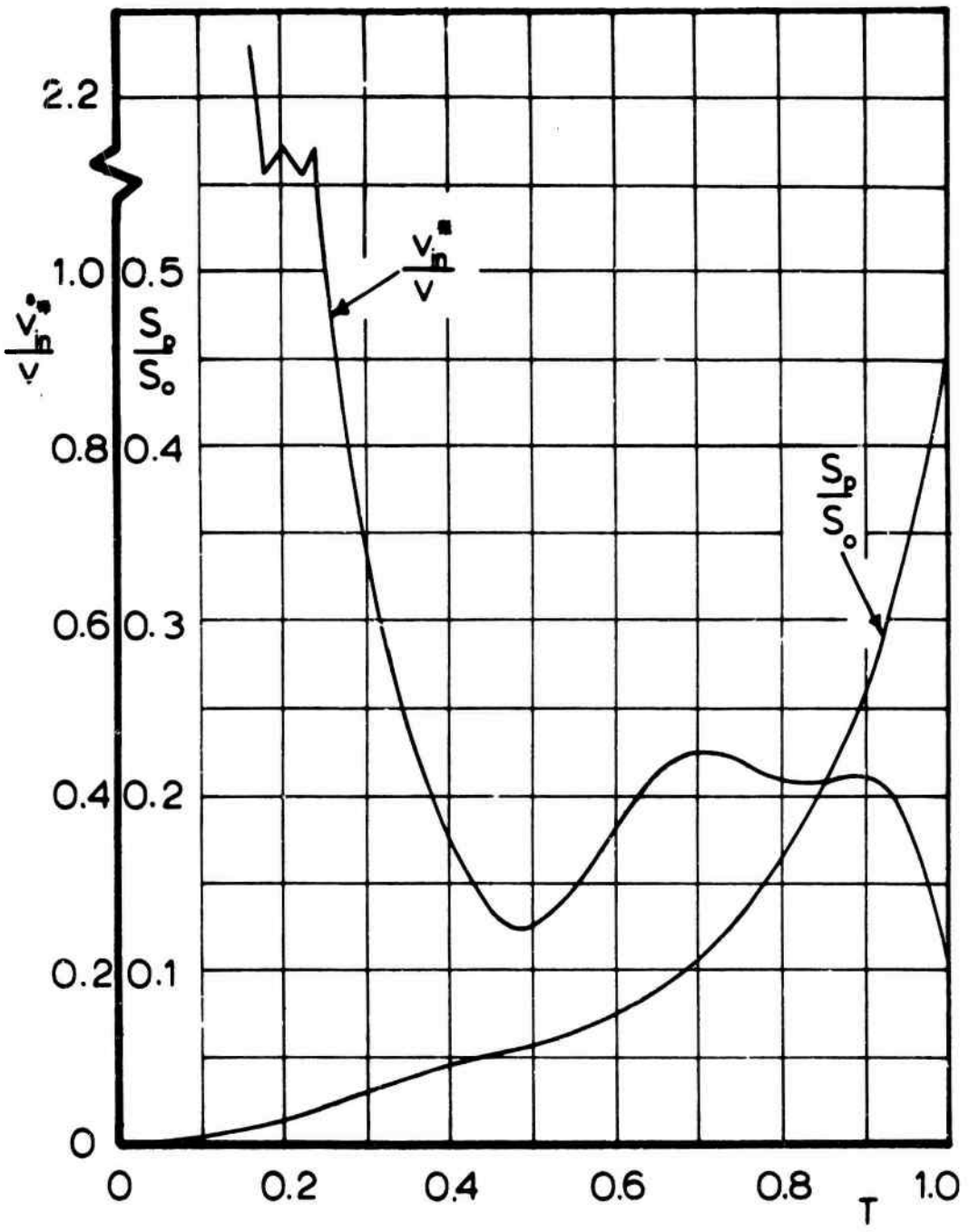

Fig 32 Area and Inflow Functions for Combination 6

TABLE VII

COEFFICIENT OF T^n FOR POLYNOMIAL APPROXIMATIONS TO AREA AND INFLOW FUNCTIONS FOR COMBINATION 6 ; NUMERICAL INPUTS FOR COMPUTER CALCULATION

n	S_p / S_o	V_{in}^* / V
0	0.0	- 2.9633770181
1	0.2587228945	212.2913975
2	- 6.7185301374	- 2572.9163183196
3	74.4319328532	14896.5925286787
4	- 417.6595768408	- 50085.2323580175
5	1423.0523996844	104458.8079783111
6	-3110.5320124241	-136903.029764805
7	4361.9076977697	109598.5899542635
8	-3771.3389266408	- 48932.3026501951
9	1822.0746849681	9330.3670098386
10	- 375.012364099	--------

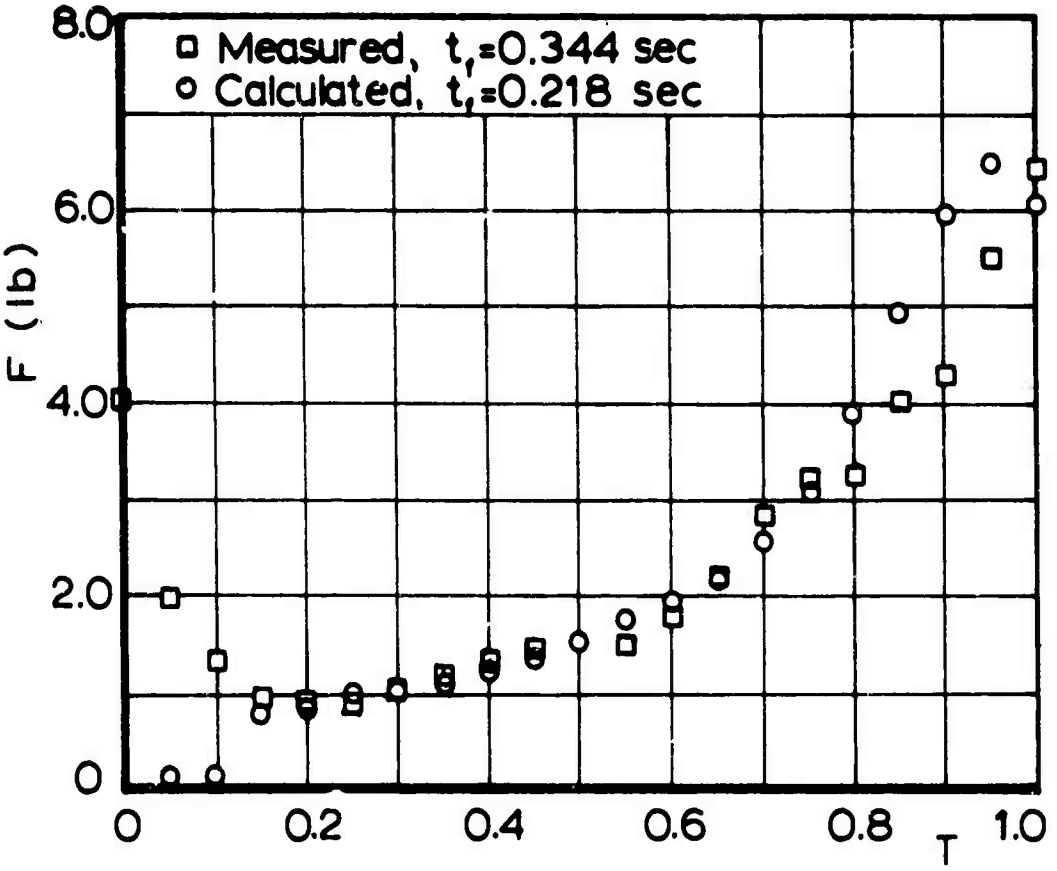

Fig 33 Calculated and Measured Average Force-Time Histories for a 3 ft Model Parachute, v_s=50 ft/sec, W_L= 0.5 lb, Combination 4

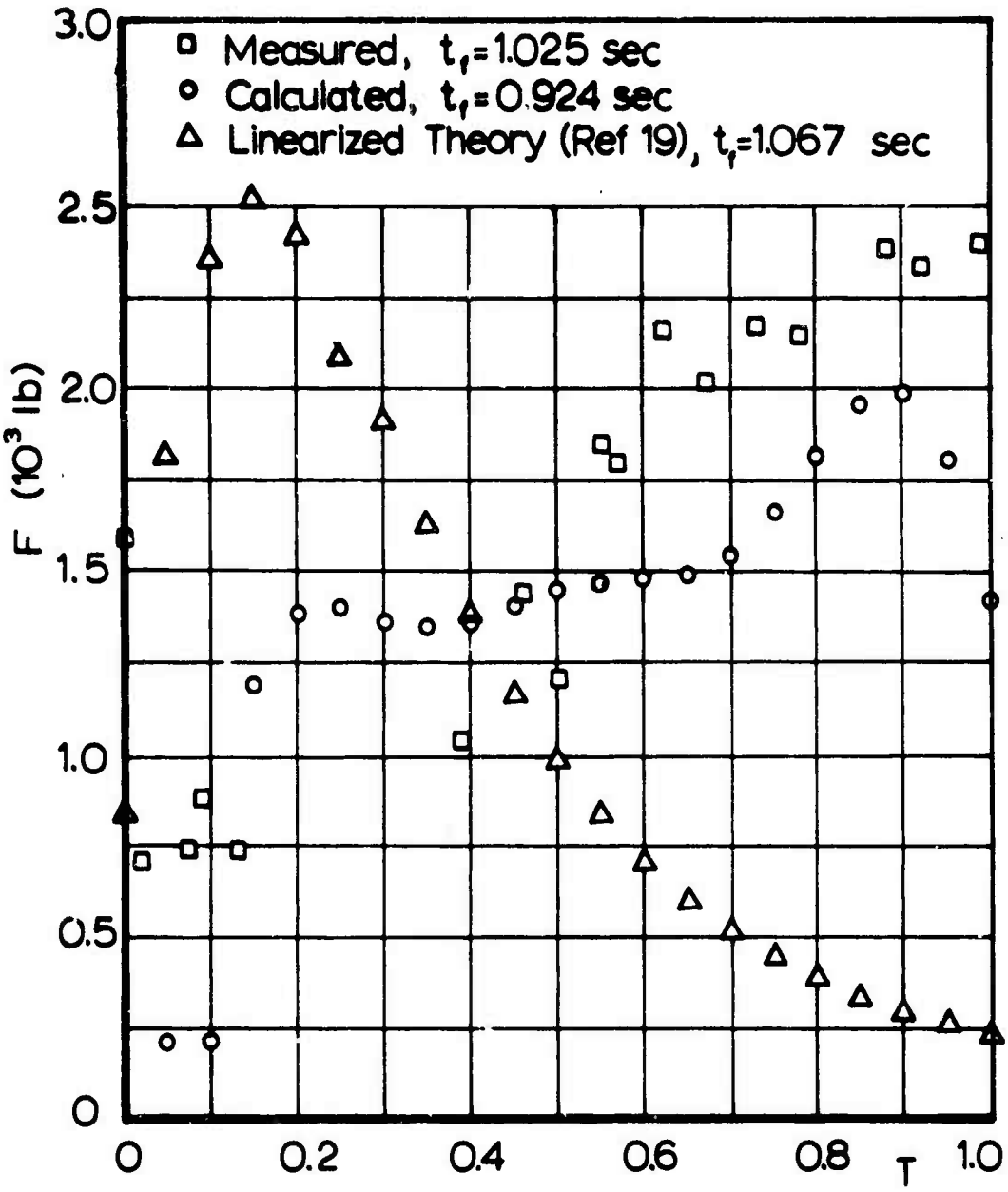

Fig 34 Calculated and Measured Force-Time Histories for a 28 ft Parachute, Test 1, v_s = 225 ft/sec, W_L = 203 lb, Combination 4

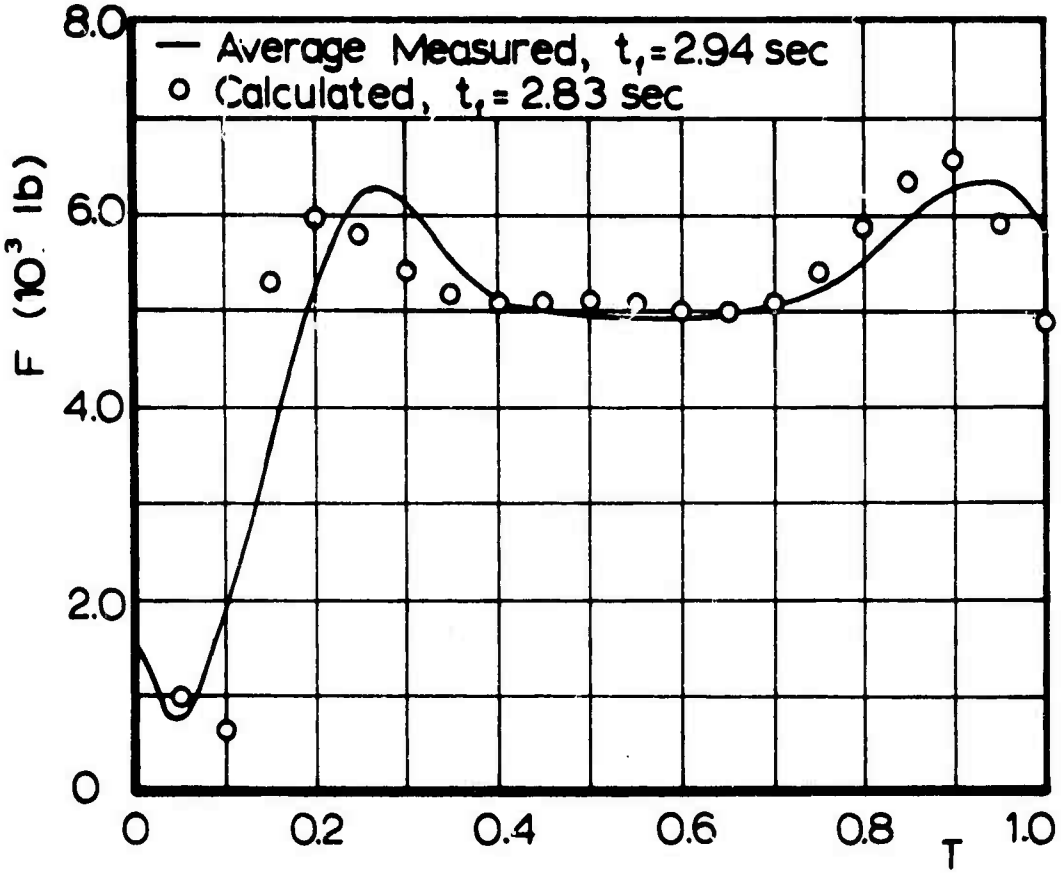

Fig 35 Calculated and Measured Average Force-Time Histories for a 64 ft, G-12D Parachute, v_s = 205 ft/sec, W_a = 2200 lb, Combination 4

VI. REFERENCES

1. Mueller, Waldemar, "Fallschirme fuer Luftfahrzuege (Parachutes for Aircraft)," Zeitschrift fuer Flugtechnik and Motorluftschiffahrt, Heft No. 20, 1927.

2. Scheubel, Franz N., Der Entfaltungsvorgang des Fallschirmes (The Opening Process of Parachutes), Deutsche Akademie der Luftfahrtforschung, ATI 23025, 1941.

3. Scheubel, Franz N., Notes on the Opening Shock of a Parachute, USAF Memorandum Report F-51-10-8507, 1946.

4. Hallenbeck, G. A., The Magnitude and Duration of Parachute Opening Shock at Various Altitudes and Air Speeds, AF Memorandum Report ENG 49-696-66, 1944.

5. O'Hara, F., "Notes on the Opening Behavior and the Opening Forces of Parachutes," Royal Aeronautical Society Journal, November, 1949.

6. Heinrich, H. G. and Bhateley, I. C., A Simplified Analytical Method to Calculate Parachute Opening Time and Opening Shock, Summer Course on Aerodynamic Deceleration, University of Minnesota, July 17-28, 1961.

7. von Karman, Theodore, Note on Analysis of the Opening Shock of Parachutes at Various Altitudes, 1945.

8. Heinrich, H. G., "Experimental Parameters in Parachute Opening Theory," Bulletin of the 19th Symposium of Shock and Vibration, 1953, Office of the Secretary of Defense, Washington, D. C. (1953).

9. Berndt, R. J., "Experimental Determination of Parameters for the Calculation of Parachute Filling Times," Jahrbuch des Wissenschaftlichen Gesellschaft fuer Luft- und Raumfahrt E.V. (WGLR), 1964, pp. 299-316.

10. Berndt, R. J. and DeWeese, J. H., The Opening Force of Solid Cloth, Personnel Type Parachutes, AIAA Paper No. 70-1167, presented at Dayton, Ohio, September, 1970.

11. Heinrich, H. G., Theory and Experiment on Parachute Opening Shock and Filling Time, Proceedings of Two Day Symposium on Parachutes and Related Technologies, Royal Aeronautical Society, London, England, 15-16 September 1971.

12. Heinrich, H. G. and Noreen, R. A., "Analysis of Parachute Opening Dynamics with Support Wind Tunnel Experiments," AIAA Journal of Aircraft, Vol. 7, No. 4, July-August 1970, pp. 341-347.

13. McEwan, A. J., An Investigation of Parachute Opening Loads, and a New Engineering Method for Their Determination, AIAA Paper No. 70-1168, presented at Dayton, Ohio, September 1970.

14. French, K. E., "Inflation of a Parachute," AIAA Journal, Vol. 1, No. 11, November 1963, pp. 2615-2617.

15. Rust, L. W., Jr., Theoretical Investigation of the Parachute Inflation Process, NVR-3887, July 1965, Northrop Corporation, Ventura Division, Newbury Park, California.

16. French, K. E., "The Initial Phase of Parachute Inflation," Proceedings of the Aerodynamic Deceleration Systems Conference, AIAA, Vol. 1, 1969, pp. 35-38.

17. Wolf, Dean, "A Simplified Dynamic Model of Parachute Inflation," AIAA Journal of Aircraft, Vol. 11, No. 1, January 1974, pp. 28-33.

18. Payne, Peter R., "A New Look at Parachute Opening Dynamics," The Aeronautical Journal, The Royal Aeronautical Society, London, Vol. 77, No. 746, February 1973, pp. 85-93.

19. Heinrich, H. G., "A Linearised Theory of Parachute Opening Dynamics," The Aeronautical Journal, The Royal Aeronautical Society, London, Vol. 76, No. 744, December 1972, pp. 723-731.

20. Heinrich, Helmut G., Noreen, Robert A. and Saari, David P., Development of a Total Trajectory Simulation for Single Recovery Parachute Systems, Volume I: Analytical Model and Computer Program Design Rationale, U.S. Army Natick Laboratories Technical Report No. TR-74-9-AD, December 1973.

21. Noreen, Robert A., and Saari, David P., Development of a Total Trajectory Simulation for Single Recovery Parachute Systems, Volume II: Calculation Procedures and Computer Program, U.S. Army Natick Laboratories Technical Report No. TR-74-9-AD (II), December 1973.

22. Uotila, Jarmo Ilmari, An Analysis of Parachute Opening Dynamics, A Thesis Submitted to the Graduate Faculty in Partial Fulfillment of the Requirements for the Degree of Master of Science, University of Minnesota, Minneapolis, Minnesota, August 1973.

23. Unpublished Data obtained from Air Force Flight Dynamics Laboratory Data Bank, Wright-Patterson Air Force Base, Ohio (R. J. Berndt and J. H. DeWeese, Project Engineers).

24. Heinrich, H. G., and Hektner, T. R., Flexibility as Parameter of Model Parachute Performance Characteristics, USAF Technical Report No. AFFDL-TR-70-53, August 1970.

25. Haak, E. L., and Thompson, R. E., Analytical and Empirical Investigation of the Drag Area of Deployment Bags, Cargo Platforms and Containers, and Parachutists, USAF Technical Report No. AFFDL-TR-67-166, July 1968.

26. McVey, D. F., and Wolf, D. F., "Analysis of Deployment and Inflation of Large Ribbon Parachutes," AIAA Journal of Aircraft, Vol. 11, No. 2, February 1974, pp. 96-103.

27. Unpublished Data Obtained from US Army Natick Laboratories, Natick, Massachusetts (E. J. Giebutowski Project Officer).

APPENDIX

Experimental Data for Large Parachutes (Ref 27)

In order to establish the necessary average information for the G-12D parachute, the behavior of the low cost, 64 ft parachute deployment phase was analyzed. The available information included force telemetry data, cinetheodolite data, and high speed films. Study of the films and the force traces showed a consistent pattern of force peaks which allowed the determination of maximum snatch force on the force traces. Correlation between the films and the corresponding cinetheodolite data provided the values for snatch velocities. For the standard G-12D parachute, which had no film coverage and hence no correlation between the force traces and velocity data, the same characteristic pattern of force peaks was evident during the deployment phase. The occurrence of maximum snatch force was then determined on the force traces by assuming the peaks represented the same events as in the case of the low cost parachute.

Having established the beginning of the time scale in this manner, average force traces for the G-12D parachute were constructed by averaging the force values and the dimensionless time values at several characteristic points of the force traces. Reported filling times were used as the basis for the dimensionless time scale. Averaged force traces were established for the two groupings of data, those with release velocities of 130 knots and those with 150 knots, and were shown in Fig 17. The average reported filling times were 2.94 sec and 3.70 sec for the 130 knot and 150 knot release velocities, respectively. Since a larger number of tests was available for the 130 knot airdrops,

the average filling time and average initial conditions for this group were used to calculate inflow functions for the G-12D parachute.

The snatch velocities for the individual airdrops were determined by examining the cinetheodolite velocity data during the deployment phase of the airdrop. The point where the velocity began to deviate markedly from the behavior of the earliest portion of the velocity-time graph was chosen as snatch. The snatch velocities determined in this way were compared with the snatch velocities for the low cost parachute airdrops (Fig 36), and in a few cases were adjusted slightly to compare more favorably with the behavior indicated by Fig 36.

The data for the 100 ft G-11A parachute with 4550 lb load did not include any reported filling times, and it was impossible to make any estimate of values for the filling times. Therefore, no averaged force-time history was constructed. In one case, film coverage of an airdrop of the same system was available with a corresponding measured force trace. This force trace had very peculiar behavior during the inflation, and this airdrop was not considered.

For the other tests, the deployment was analyzed, and a characteristic behavior of the force trace during this period was established allowing the determination of the instant of snatch by examination of the force traces. The corresponding cinetheodolite data was correlated with the force traces, and the snatch velocities were determined.

The G-11A airdrops with 5410 lb included reported filling times and snatch velocities and these data have been used in the preceding text.

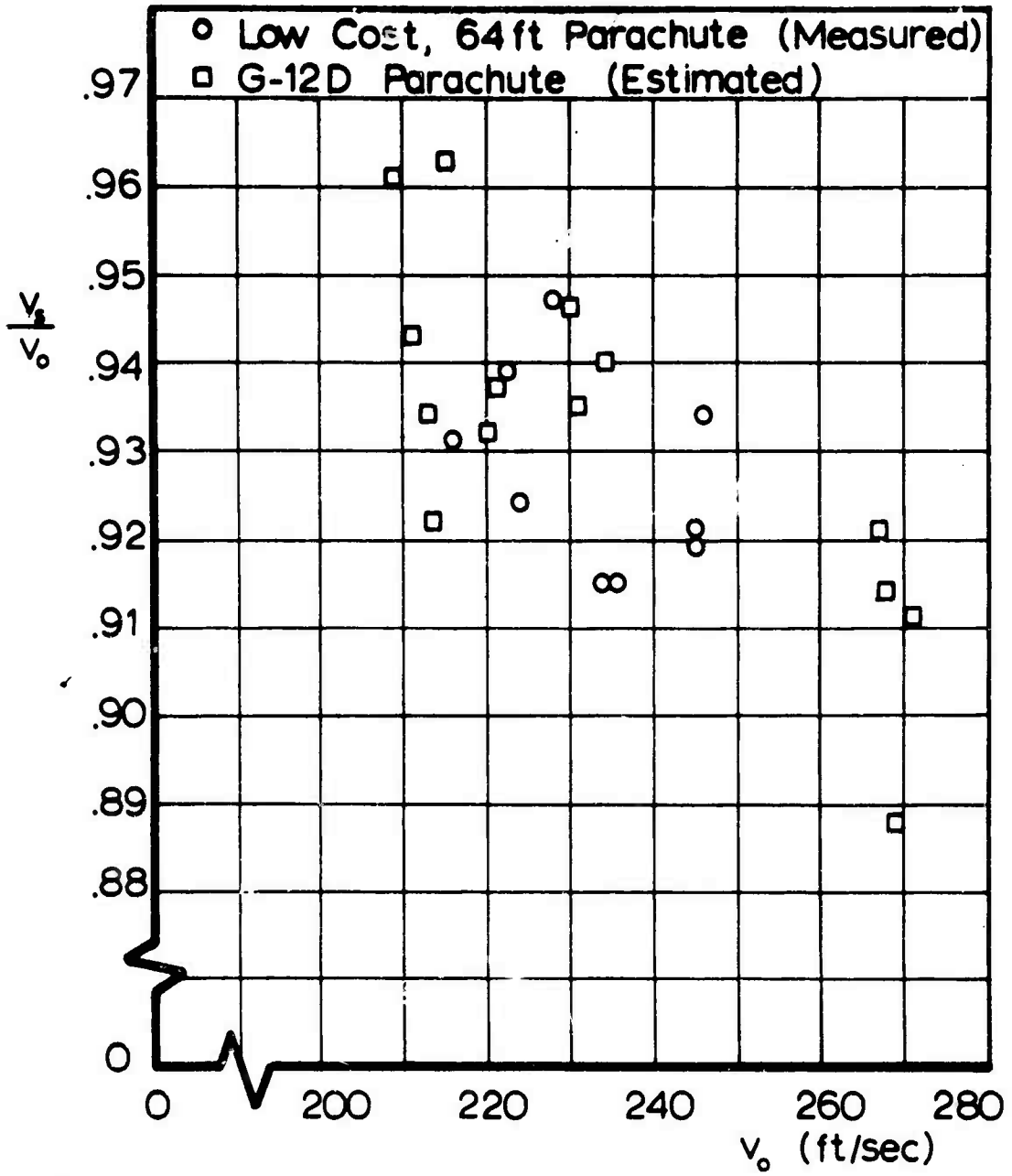

Fig 36 Estimation of Snatch Velocities for 64 ft, G-12D Parachute